

**UCLA**

**UCLA Electronic Theses and Dissertations**

**Title**

Processable Conducting Polyaniline, Carbon Nanotubes, Graphene and Their Composites

**Permalink**

<https://escholarship.org/uc/item/7mn0b5d8>

**Author**

Wang, Kan

**Publication Date**

2014

Peer reviewed|Thesis/dissertation

UNIVERSITY OF CALIFORNIA  
Los Angeles

Processable Conducting Polyaniline, Carbon Nanotubes,  
Graphene and Their Composites

A dissertation submitted in partial satisfaction of the  
requirements for the degree of Doctor of Philosophy in  
Chemistry

By

Kan Wang

2014

© Copyright by

Kan Wang

2014

## ABSTRACT OF THE DISSERTATION

Processable Conducting Polyaniline, Carbon Nanotubes,  
Graphene and Their Composites

by

Kan Wang

Doctor of Philosophy in Chemistry

University of California, Los Angeles, 2014

Professor Richard B. Kaner, Chair

Good processability is often required for applications of conducting materials like polyaniline (PANI), carbon nanotubes (CNTs) and graphene. This can be achieved by either physical stabilization or chemical functionalization. Functionalization usually expands the possible applications for the conducting materials depending on the properties of the functional groups. Processable conducting materials can also be combined with other co-dissolving materials to prepare composites with desired chemical and physical properties.

Polyanilines (PANI) doped with dodecylbenzenesulfonic acid (DBSA) are soluble in many organic solvents such as chloroform and toluene. Single wall carbon nanotubes (SWCNTs) can be dispersed into PANI/DBSA to form homogeneous solutions. PANI/DBSA functions as a conducting surfactant for SWCNTs. The mixture can be

combined with two-parts polyurethanes that co-dissolve in the organic solvent to produce conducting polymer composites. The composite mixtures can be applied onto various substrates by simple spray-on methods to obtain transparent and conducting coatings.

Graphene, a single layer of graphite, has drawn intense interest for its unique properties. Processable graphene has been produced in N-methyl-2-pyrrolidone (NMP) by a one-step solvothermal reduction of graphite oxide without the aid of any reducing reagent and/or surfactant. The as-synthesized graphene disperses well in a variety of organic solvents such as dimethylsulfoxide (DMSO), ethanol and tetrahydrofuran (THF). The conductivity of solvothermal reduced graphite oxide is comparable to that of hydrazine reduced graphite oxide.

Attempts were made to create intrinsically conducting glue comparable to mussel adhesive proteins using polyaniline and graphene. Mussels can attach to a variety of substrates under water. Catechol residue in 3,4-dihydroxyphenylalanine (L-DOPA) is the key to the wet adhesion. Tyrosine and phosphoserine with primary alkyl amine groups also participate in adhesion. A novel water soluble synthetic mussel adhesive containing both catechol and amine groups are synthesized in a simple approach. A polyallylamine backbone is used to take the place of the polyamide chain. Catechol is appended to the backbone as the key cross-linking group. Compared to polyallylamine, poly[N-(3,4-dihydroxybenzylidene)allylamine] exhibits good adhesion under alkaline water due to moderate cross-linking. When exposed to cross-linkers, this synthetic mussel adhesive can form a hydrogel at a very low concentration.

Various methods were tried to attach catechol group onto polyaniline and graphene to make synthetic conductive mussel adhesive. Although the chemistry proved to be successful, the material doesn't show great adhesion to selected substrates probably due the nature of the backbone and difficulties associated with its processability.

The dissertation of Kan Wang is approved.

Yang Yang

Jeffrey I. Zink

Yves F. Rubin

Richard B. Kaner, Committee Chair

University of California, Los Angeles

2014

# TABLE OF CONTENTS

## **Chapter 1** Introduction to Polyaniline

1.1 Introduction to Conducting Polymers

1.2 Basics of Polyaniline

1.3 Processability of Polyaniline

1.4 Polyaniline Derivatives

1.5 Applications

1.6 Conclusions

1.7 References

## **Chapter 2** Dispersions of Polyaniline/Carbon Nanotubes in Organic Solvents as Conductive Fillers for Polyurethane

2.1 Introduction

2.2 Experimental Section

2.3 Results and Discussion

2.4 Conclusions

2.5 References

## **Chapter 3** A Novel Water-Soluble Synthetic Mussel Adhesive

3.1 Introduction

3.2 Experimental Section

3.3 Results and Discussion

3.4 Conclusions

3.5 References



## **Chapter 4** Polyaniline-Based Electrically Conductive Synthetic Mussel Adhesive

4.1 Introduction

4.2 Polyaniline doped with 3,4-dihydroxybenzenesulfonic acid

4.3 N-alkylation of polyaniline with catechol containing functional groups

4.4 Poly(2,3-dihydroxyaniline-co-aniline)

4.5 Catechol Functionalized Graphene

4.6 Conclusions

4.7 References

## **Chapter 5** Solvothermal Reduced Graphene Oxide Dispersions in Organic Solvents

5.1 Introduction

5.2 Experimental Section

5.3 Results and Discussion

5.4 Conclusions

5.5 References

## LIST OF FIGURES

### Chapter 1 Introduction to Polyaniline

Figure 1.1 Structures of common conducting polymers in their neutral states.

Figure 1.2 Evolution of p-type conducting polymer band structure. Left: the formation of a polaron at a low doping level. Middle: bipolaron formation at a moderate doping level. Right: formation of bipolaron bands at a high doping level.

Figure 1.3 Synthesis of conducting polyaniline by chemical oxidation. The synthesized product is the doped form of emeraldine state. The emeraldine state can be fully oxidized and reduced to produce unstable pernigraniline and leucoemeraldine. The picture is published in *Acc. Chem. Res.* 2009, 42, 135.

Figure 1.4 By choosing a proper acid/solvent pair, the compact coiled polyaniline expands due to the electrostatic repulsion effect.

Figure 1.5 Self-doped polyaniline by sulfonation on polymer chains. The sulfonic groups on the polymer backbone protonate the imines to produce the conducting form. The negatively charged sulfonates stabilize the polymer in neutral or alkaline water solution.

Figure 1.6 Synthesis of polyaniline in a rapidly mixed reaction a) The oxidant (open circles) dopant solution is quickly added into the aniline (solid circles) dopant solution and mixed. b) A homogenous solution is obtained where all the aniline and oxidant molecules are evenly distributed, thus leading to fast polymerization across the entire solution. c) Since all the reactants are consumed in the formation of nanofibers, secondary growth is suppressed. The right picture shows the nanofiber structure under SEM. Picture is published in *Angew. Chem.* 2004, 116, 5941.

Figure 1.7 (A) An SEM image of a flash welded film with an asymmetric cross section (B) The actuation of the as-formed asymmetric film upon exposure to an acid or base. Picture is published in *Acc. Chem. Res.*, 2009, 42, 135.

### Chapter 2 Dispersions of Polyaniline/Carbon Nanotubes in Organic Solvents as Conductive Fillers for Polyurethane

Figure 2.1 Process to prepare polyaniline/DBSA/SWCNT composite in an organic solvent. The final composite is stable with no visible particles.

Figure 2.2 (a) From left to right: solutions of polyaniline/DBSA with 0%, 25%, 50% and 100% carbon nanotube loadings in chloroform. The solutions are clear without any visible particles. The rightmost one is carbon nanotubes in DBSA only (without polyaniline). (b) Gel forms at over 200% carbon loading. (c) After dilution, the carbon nanotubes at 100% loading precipitates (left), while the 25% loading solution (right) is still clear and stable.

Figure 2.3 (a) From left to right: spin-coated thin films from polyaniline/DBSA solution with 0%, 25%, 50% and 100% SWCNT loading. (b) Sheet resistance of spin-coated films with different SWCNT loading. (c) SEM images of polyaniline/DBSA/SWCNT composites in chloroform (left) and toluene (right). (d) Polyaniline/DBSA solution without SWCNT (right) and with 25% SWCNT (left) drop-cast to obtain thick films. After rinsing with water, the film without the SWCNTs breaks into pieces due to its poor mechanical properties.

Figure 2.4 Left: a low magnitude picture of polyurethane composite. Carbon nanotubes are connected to form conductive pathways. Right: A zoomed-in picture of milky circles in the left picture. These white bands are composed of bundles of partially aligned carbon nanotubes. They are probably caused by solvent evaporation.

Figure 2.5 (a) Thin films of polyurethane films incorporated with polyaniline/DBSA/0.5SWCNT. The loading percentages from left to right are 10%, 20%, 30% and 40%. (b) Visible transmittance spectrum of 30% loaded film.

### Chapter 3 A Novel Water-Soluble Synthetic Mussel Adhesive

Figure 3 (a) Mussel is connected to a mica sheet using byssal threads. (b) Schematic drawing of a byssal thread attached to a substrate. Different mussel foot proteins are located at different places. The picture has been adapted from Reference 4.

Figure 3.2 L-DOPA forms strong adhesive bonds by bidentate hydrogen bonding and metal/metal oxide coordination (left). L-DOPA that has been oxidized to L-DOPA quinone can be reduced by thiol-containing groups to form adhesive bonds (center). L-DOPA quinone can also participate in cohesive oxidative crosslinking and metal chelation to form the bulk material (right). The picture is adapted from Reference 5.

Figure 3.3 <sup>1</sup>H-NMR spectrum of synthetic mussel adhesive. The ratio between d and h is approximately 1.5. The slight difference is probably caused by some boron adduct formation during the reduction.

Figure 3.4 (a) Strong interaction between OH and NH<sub>2</sub> precipitates the imine product. (b) The anionic borate complex solubilized polymer. (c) The positively charged final product is soluble in water.

Figure 3.5 (a) Adhesion test of the mussel adhesive mimic with (right) and without (left) an oxidative cross-linker. (b) Adhesion test of polyallylamine with (right) and without (left) an oxidative cross-linker. (c) Synthetic mussel adhesive can hold a glass vial filled with water. (d) Polyallylamine can also hold a glass vial. (e) Oxidative cross-linking of catechol groups weakens the adhesion. (f) Polyallylamine (left) dissolves in alkaline water, while the synthetic mussel adhesive still holds the two glass slides together.

Figure 3.6 (a) Solution of mussel mimic and borate salt in water before dialysis; the nature of the borate salt makes the solution quite alkaline. (b, c) After overnight dialysis, the polymer solution becomes a homogeneous hydrogel. (d) The mechanism of hydrogel formation: from a mono-catechol complex at high pH (left) to a bi-catechol complex at moderate pH (middle) and finally to a borate-free catechol at low pH (right).

Figure 3.7 (a) When a 5% polymer solution is exposed to ammonia vapor, it becomes a red gel within seconds. (b) The formed hydrogel is then cut into two pieces. (c) When brought together the two halves fuse within minutes. (d) The self-healed hydrogel can then be lifted up. (e) The likely mechanism for hydrogel formation.

Figure 3.8 Left: dried polymer film. Right: when the film is dipped into water, it swells to form a gel.

## Chapter 4 Polyaniline-Based Electrically Conductive Synthetic Mussel Adhesive

Figure 4.1  $^1\text{H}$  NMR spectrum of 3,4-dihydroxybenzenesulfonic acid ( $\text{CD}_3\text{OD}$ ).

Figure 4.2  $^1\text{H}$  NMR spectrum of N-alkylated polyaniline in  $\text{DMSO-d}_6$ . The solubility of the polymer is very low and the soluble part shows that the degree of substitution is only 7%.

Figure 4.3  $^1\text{H}$  NMR spectrum of 4-aminocatechol HCl salt.

Figure 4.4 Left: catechol functionalized graphene exhibits its characteristic reduction peak in a CV curve. The functionality increases the dispersibility of graphene in water, but decreases the conductivity. Right: a control experiment shows no redox peaks. The conductivity is the same as CCG, because of no chemical modification. Graphene precipitates due to the salt effect.

Figure 4.5 Force-distance curves describing a single approach-retract cycle of the AFM tip. The AFM tip approaches the sample surface (A). The initial contact between the tip and the surface is mediated by the attractive van der Waals forces (contact) that lead to an attraction of the tip toward the surface (B). Hence, the tip applies a constant and default force upon the surface that leads to sample indentation and cantilever deflection (C).

Subsequently, the tip tries to retract and to break loose from the surface (D). Various adhesive forces between the sample and the AFM tip, however, hamper tip retraction. These adhesive forces can be taken directly from the force-distance curve (E). The tip withdraws and loses contact to the surface upon overcoming of the adhesive forces (F). The original picture was published in *J Cell Sci.* **118**, 2881-2889.

## Chapter 5 Solvothermal Reduced Graphene Oxide Dispersions in Organic Solvents

Figure 5.1 A proposed graphite oxide structure. Picture adopted from *J. Phys. Chem. B* 1998, **102**, 4477.

Figure 5.2 The preparation and purification of solvothermally reduced graphene oxide (SRGO) to create homogeneous colloidal dispersions of SRGO sheets.

Figure 5.3(a) AFM image of SRGO sheets; (b) corresponding AFM height profile from (a) indicates a 0.93 nm sheet thickness. (c) SEM images of SRGO sheets indicate well-dispersed sheets after deposition on Si substrate; inset shows a highly magnified single sheet of SRGO.

Figure 5.4 (a) XRD of graphite (top), graphite oxide (middle), reduced graphite oxide (bottom). (b) Thermal gravimetric analysis (TGA) plot shows a normalized remaining mass of graphite oxide, graphite, and reduced graphite oxide heated under argon.

## LIST OF SCHEMES

### **Chapter 3** A Novel Water-Soluble Synthetic Mussel Adhesive

Scheme 3.1 (i) Polyallylamine hydrochloride reacts with NaOH in methanol for 24 hours at r. t. to produce polyallylamine base solution. (ii) Polyallylamine base reacts with dihydroxybenzaldehyde in methanol for 2 hours to form Schiff's base. (iii) Schiff's base is reduced by NaBH<sub>4</sub> in methanol. (iv) The product is purified by dialysis against 1mM HCl.

### **Chapter 4** Polyaniline-Based Electrically Conductive Synthetic Mussel Adhesive

Scheme 4.1 Synthesis of 3,4-dihydroxybenzenesulfonic acid and the doping of polyaniline emeraldine base.

Scheme 4.2 N-alkylation of polyaniline. To maximize the degree of substitution, polyaniline is first reduced to the leucoemeraldine state. The amine group is deprotonated by dimethyl ion and functionalized by an alkyl halide. The deprotection of the catechol group is carried out in a boron tribromide solution.

Scheme 4.3 Synthesis of poly(2,3-dihydroxyaniline-co-aniline).

Scheme 4.4 Catechol-4-diazonium salt can be prepared in HCl with NaNO<sub>2</sub>. It can react with the sp<sup>2</sup> regions of chemically converted graphene to attach catechol groups onto the graphene surface.

## LIST OF TABLES

### **Chapter 2** Dispersions of Polyaniline/Carbon Nanotubes in Organic Solvents as Conductive Fillers for Polyurethane

Table 2.1 Sheet Resistances of Polyurethane Composite Films Cast by Spray-Coating

### **Chapter 4** Polyaniline-Based Electrically Conductive Synthetic Mussel Adhesive

Table 4.1 Composition and sheet resistance of poly(2,3-methoxyaniline-co-aniline). DMOA is short for 2,3-dimethoxyaniline. The ratio of the two monomers was calculated from the proton NMR spectrum.

### **Chapter 5** Solvothermal Reduced Graphene Oxide Dispersions in Organic Solvents

Table 5.1 Electrical Conductivities SRGO Paper and Hydrazine Reduced Graphite Oxide

Table 5.2 Atomic Composition of SRGO and Hydrazine RGO Measured by XPS

## ACKNOWLEDGEMENTS

First I would like to acknowledge Professor Richard Kaner for letting me join your very diverse and creative group. Ric, I think you are the best teacher I have ever met in my life. In the mean time, I want to say you are also a nice PI, a genius scientist, a fantastic speaker and a great person. I feel really lucky to be your student in my graduate study. What I learn from you will benefit my whole life.

I would also like to thank my wife, thanks for your support and encouragement throughout my graduate study. No matter what kind of difficulty I meet, you are always here with me and help me. I'm sure we will walk through our lives hand in hand. And thanks to my mother and father. Your love is the best support!

Also I want to thank the Kaner group. Thanks for all your help since my first day in the lab. Thank you to Sergey for your guide and help since my summer research as an undergraduate student. And thank you Tom. It's a great pleasure to work with you on the conductive coating project. With the help of your creative ideas, we can achieve our three-year goal in just one year! And thanks to everyone in the lab for your generous help. I feel like I'm in a warm family.

At last I would like to thank all the teaching instructors I've been worked with, especially Dr. Pang (and of course Prof. Kaner). I had a great time with all of you.



## VITA

- 2005-2009 Bachelor of Science  
Chemistry  
University of Science and Technology of China
- 2009-present Teaching Assistant  
Department of Chemistry and Biochemistry University of  
California, Los Angeles  
Los Angeles, California
- 2009-present Research Assistant  
Department of Chemistry and Biochemistry  
University of California, Los Angeles  
Los Angeles, California
- 2008-present The Cross-disciplinary Scholars in Science and Technology  
(CSST) program  
Department of Chemistry and Biochemistry  
University of California, Los Angeles  
Los Angeles, California

# Chapter 1 Introduction to Polyaniline

## 1.1 Introduction to Conducting Polymers

Conventional organic polymers like plastics and rubber are typically insulating. Conducting polymers have received a lot of attention since the discovery of polyacetylene in the 1970s by Hideki Shirakawa, Alan Heeger, and Alan MacDiarmid. In 2000, the Nobel Prize in chemistry was awarded to them for their discovery of electrically conducting polymers.

The process to make a polymer conductive is called ‘doping’ in analogy with inorganic semiconductors. However the process (which is actually redox chemistry) is quite different from the corresponding inorganic semiconductors. For conducting polymers, oxidation of the polymer leads to p-type doping, while the use of a reducing agent leads to n-type doping. This can explain why conducting polymers are always  $\pi$ -conjugated polymers: the  $\pi$  electrons can be removed (p-type doping) and added (n-type doping) to the polymer without much disruption of the  $\sigma$  bonding which forms the backbone of the polymer. The common conducting polymers are shown in Figure 1.1. The doping process can be achieved by either chemical or electrochemical oxidation/reduction.

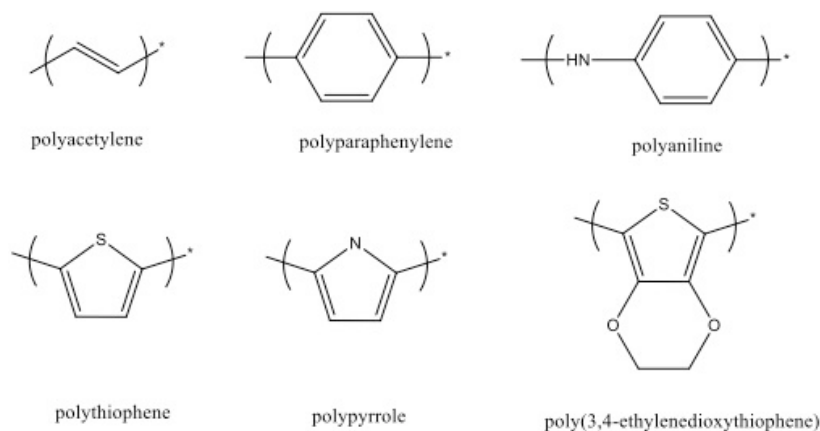


Figure 1.1 Structures of common conducting polymers in their neutral states.

Like inorganic semiconductors, the doping process increases the conductivity of the polymer greatly from  $<10^{-10}$  to  $>10^2$  S/cm. For most conducting polymers such as polypyrrole, polythiophene and polyaniline, the doping causes the energy distortion of the polymer band structure through the formation of polarons and bipolarons as shown in Figure 1.2.[1] Unlike their inorganic analogs, the doping level for conducting polymers is very high (often above 20%), while the doping level for inorganic semiconductors are usually less than one percentage.

The total conductivity of a conducting polymer in its doped form is a sum of its intrachain (intramolecular) and interchain (intermolecular) conductivity. The former includes the number of defect sites and the extent of conjugation. The latter depends on conjugated cross-links between polymer chains and the degree of oriented micro/macro crystal domains.

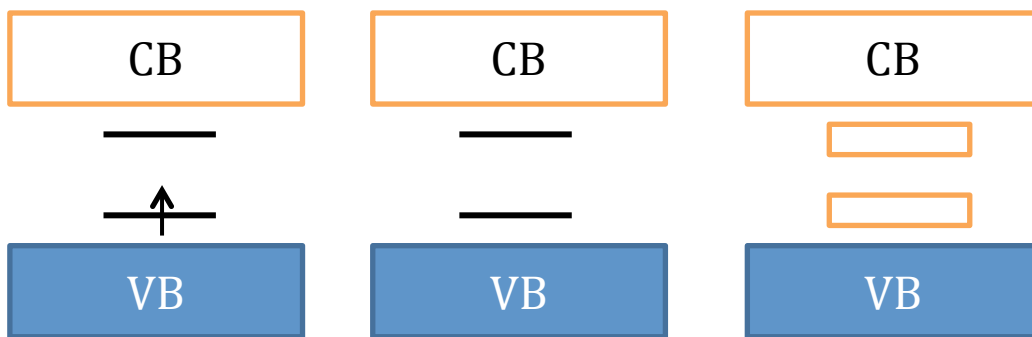


Figure 1.2 Evolution of p-type conducting polymer band structure. Left: the formation of a polaron at a low doping level. Middle: bipolaron formation at a moderate doping level. Right: formation of bipolaron bands at a high doping level.

Most conducting polymers are actually intractable due to the strong aromatic interaction between the polymer chains. Many attempts have been made to improve the processability of these polymers. These methods include special solvents, soft templates, self-doping and the use of solubilizing groups.[2] More details for polyaniline processability is discussed in Section 1.3. Thanks to all these efforts to induce processability as well as other physical property characterizations of the conducting polymers, they are now available in forms that are highly conductive, soluble in common solvents, thermally stable and mechanically strong.

The properties of conducting polymers gives them advantages over other materials in a wide range of applications such as batteries, supercapacitors, light emitting diodes (LEDs), sensors, transistors, photovoltaics and more.[2] Some recent applications of polyaniline will be briefly discussed in Section 1.5. In recent years numerous articles have been published on each topic of the aforementioned applications as well as the synthesis and improvement of new and existing conducting polymers. So I will not be surprised if one day these organic conductors replace current materials and dominate future markets.

## **1.2 Basics of Polyaniline**

Among all the conducting polymers, polyaniline is a very special type. It was discovered 150 years ago [3], one hundred years ahead of the history of conducting polymer. Since 1980s, the publication on polyaniline becomes greater and greater due to the rediscovery of the high conductivity of polyaniline. The study of polyaniline has become one of the most studied conducting polymers in the past decades. Besides conductivities, polyaniline

has some other advantages over its competitors. First, the monomer aniline is very cheap as a basic industrial precursor to many chemicals. And the synthesis of polyaniline is usually achieved through a very simple and inexpensive chemical oxidation process. Aqueous and organic solvent solution of highly conducting polyaniline can also be prepared on industrial scale through inexpensive ways. Second, polyaniline is air stable compared to the much more conducting but air sensitive polyacetylene. It is also thermally stable up to 250 °C [4]. Third, polyaniline is a rich chemistry polymer. Aniline derivatives with various functional groups are commercially available at low cost. The polymerization and copolymerization of these monomers can be carried out in the same way as polyaniline. Polyaniline itself can also be grafted with many functional groups through post modification. Fourth, the doping process of polyaniline is quite unique. The doping/dedoping of polyaniline is an acid/base reaction (Figure 1.3) whereas other conducting polymers go through a redox reaction. Doped polyaniline with different acids can achieve conductivity >100S/cm while the conductivity of dedoped neutral form falls in the range of insulator. The nature of acid also plays a great role in the physical properties of the polymer.

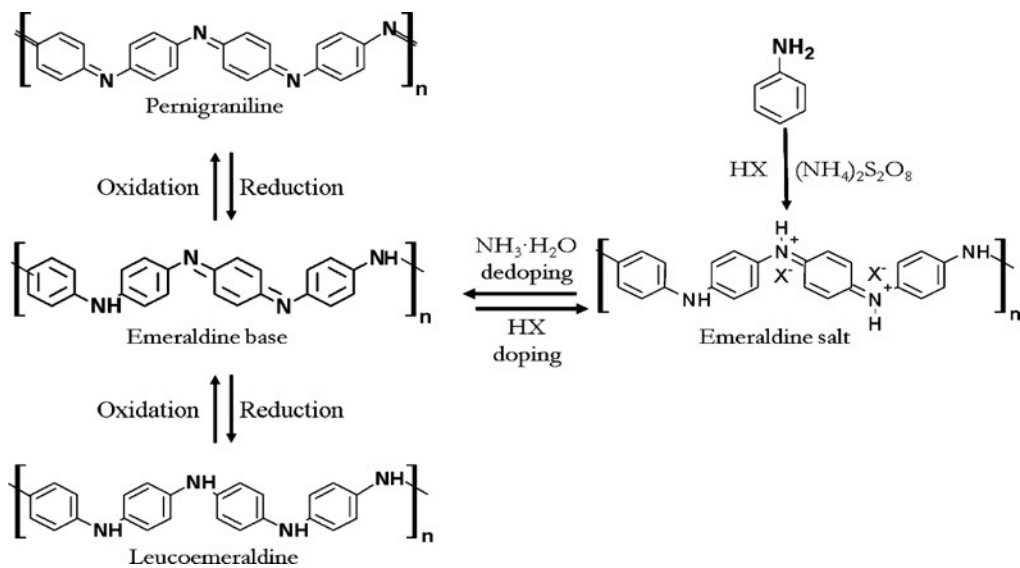


Figure 1.3 Synthesis of conducting polyaniline by chemical oxidation. The synthesized product is the doped form of emeraldine state. The emeraldine state can be fully oxidized and reduced to produce unstable pernigraniline and leucoemeraldine. The picture is published in *Acc. Chem. Res.* 2009, 42, 135.

Polyaniline can be synthesized through a simple one-step oxidative polymerization as is shown in Figure 1.3. The reaction is carried out in an acidic medium with a proper oxidizing agent. The aniline monomers are first oxidized to radical cations, which leads to the formation of dimer. Because of its lower oxidation potential, the dimer is immediately oxidized to yield the corresponding cations, which will attack another aniline monomer by electrophilic reaction. And the reaction proceeds to the final polymer.[5] Conventionally the polymerization is carried out at 0-5 °C with slowly addition of oxidant. With the addition of salt like LiCl, polyaniline can be synthesized at sub-zero temperature.[6] The lower temperature and the additional salt increase the dielectric constant of the solution and lead to the high molecular weight polymer. (160kDa at -25°C vs. 20kDa at 18 °C) Acidic condition is required for the synthesis of polyaniline. The structure obtained under alkaline condition is confirmed to be phenazine-like oligomers rather than the conducting polymers.[7]

The synthesized conducting polyaniline is half oxidized which is called the emeraldine state. Only the emeraldine state exhibits conductivity. The dedoped base form of the emeraldine polyaniline is blue. Upon doping with an acid, the color of the polymer turned into green and becomes conductive. As is shown in Figure 1.3, there are three oxidation states for polyaniline. The most stable state is the emeraldine state, in which half of the units are oxidized, and the polymer chain is compromised of both benzoid and quinoid

(or half amine and half imine in terms of nitrogen). The fully reduced form (leucoemeraldine) and fully oxidized form (pernigraniline) are not stable in air and will gradually transform into the emeraldine state. In the case of leucoemeraldine, a slow oxidation takes place in the presence of oxygen; while the pernigraniline lowers its oxidation state turns into the emeraldine state. Pernigraniline can be synthesized by the controlled oxidation of emeraldine base by m-chloroperbenzoic acid [8]. Leucoemeraldine polyaniline can be prepared by reduction of emeraldine base by hydrazine or phenylhydrazine.[9] Although leucoemeraldine is not quite air stable, it's important for the synthesis of functionalized polyaniline.

### **1.3 Processability of Polyaniline**

As mentioned before, processability is one of the key properties for conducting polymers. Great progress has been made since the rediscovery of this conducting polymer.

#### *Emeraldine Base Solution*

The emeraldine base form of polyaniline has been found soluble in N-methylpyrrolidinone (NMP) and other polar solvents.[10, 11] (Some argue that there is no true solution but only the very fine dispersion of polyaniline.) A solution of polyaniline in NMP gels over time due to the strong interchain hydrogen bonding [11]. The time of gelation decreases as the concentration and the molecular weight increase. The dropcast film from this NMP solution can be stretched through simultaneous heat treatment to produce oriented, partially crystalline film. The conductivity increases from 8S/cm for unstretched film to a maximum 216S/cm for stretched film due to the increased intermolecular and intermolecular electron mobility.[11] This stretched film out of NMP solution however can no longer dissolve back anymore because of the crystallinity.

### *Doped Polyaniline Solution*

In 1992, Yong Cao [12] reported doped polyaniline is soluble in many common organic solvents with the use of functionalized strong acids. The choose of solvent/acid pairs is very important. These carefully chosen acids act as both dopants and surfactants. For example, dodecylbenzenesulfonic acid has a long alkyl chain and this leads to the solubility of polyaniline in many less polar solvents such as toluene, xylenes and chloroform. This conducting polymer solution can be blended with a variety of polymers that are also compatible with the solvent at the desired ratio. The conducting polymer blends can be fabricated into shapes by solution processing methods. This protonated polyaniline solution is in the conducting form and requires no more post treatment. In m-cresol/camphorsulfonic acid system, 1S/cm can be obtained with only 2% loading of polyaniline.

It's amazing that the film cast from the above polyaniline solution shows conductivity in the range 100-400 S/cm, nearly two orders higher than the conventional polyaniline film. The concept of 'secondary doping' is introduced to explain this phenomenon.[13, 14] As mentioned before, the solubility is a big problem for most conducting polymers because of the strong polymer-polymer interactions. Thus the undoped polyaniline chain tends to interact with each other to form a 'compact coil' conformation. However, in a 'good solvent', the doped polyaniline can dissolve and generate the positively charged polymer chains and the negatively charged dopant ions. The electrostatic repulsion between the polymer chains will expand polyaniline to 'expanded coil' conformation. (Figure 1.4)



This will increase both the intramolecular conductivity (less  $\pi$ -conjugation defects) and the intermolecular conductivity (more crystallinity of the bulk polymer).

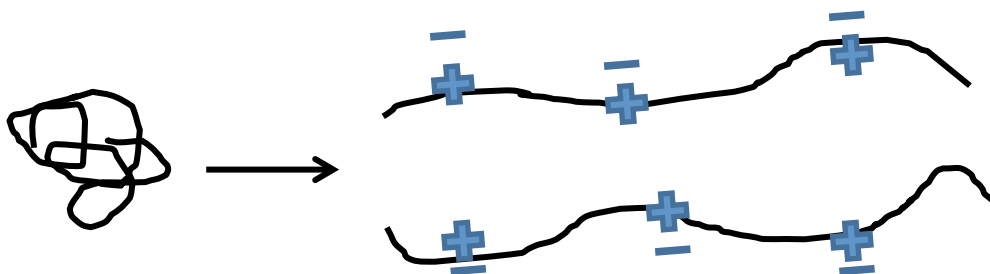


Figure 1.4 By choosing a proper acid/solvent pair, the compact coiled polyaniline expands due to the electrostatic repulsion effect.

#### *Self-doped Polyaniline Solution*

Just like DBSA can dissolve polyaniline in less polar solvents because of ‘like dissolves like’, polyaniline bears negatively charged functional groups can dissolve in water. This kind of polyaniline derivatives is called ‘self-doped’ polyaniline. Typically, the self-doped polyaniline is synthesized by sulfonation of emeraldine base in concentrated sulfuric acid or chlorosulfonic acid [15]. (Figure 1.5) The sulfonic groups on the polymer chain stabilize polyaniline in water as well as dope the polymer chain by itself. Thanks to this self-doping effect, the synthesized polymer is pH dependent when pH is less than 7. Based on the same mechanism, many other sulfonic groups bearing polyaniline derivatives are synthesized [16, 17]. Although this kind of polymers can increase the solubility, the electron withdrawing sulfonic group will destruct the conjugation system and thus lower the conductivity more or less.

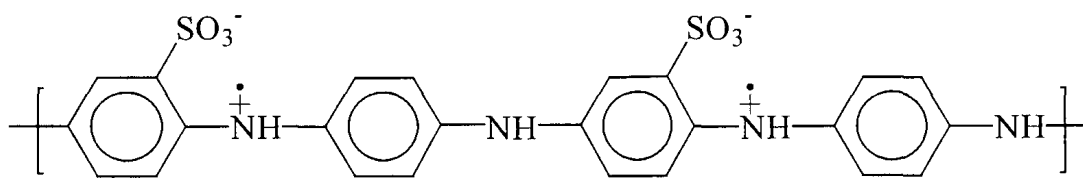


Figure 1.5 Self-doped polyaniline by sulfonation on polymer chains. The sulfonic groups on the polymer backbone protonate the imines to produce the conducting form. The negatively charged sulfonates stabilize the polymer in neutral or alkaline water solution.

#### *Aqueous Dispersion of Polyaniline Nanofibers*

Among all the solvents, water is the least toxic one and is preferred in more and more chemistry. Although polyaniline can be dispersed in water by functionalization of sulfonic groups and other polar functional group, the conductivity will decrease dramatically in most cases. So it will be very exciting to prepare a true aqueous dispersion of pristine polyaniline fibers. Among all the surfactants or soft templates, polymeric acids such as polystyrenesulfonic acid can be used as both surfactant and dopant to obtain a stable aqueous dispersion. DBSA with a much smaller molecular size is a better choice in terms of conductivity.[18] Our group reported a more general and facile synthesis.[19, 20] In this breakthrough method, uniform and well-dispersed polyaniline nanofibers can be made by a simple interfacial polymerization or rapid-mix polymerization. (Figure 1.6) In a typical rapidly mixed reaction, aniline monomer and oxidant such as ammonium persulfate are dissolved separately in a given acid solution. The two solutions are mixed at once and shaken for seconds. After 3-5 min, the green polyaniline nanofibers form homogeneously in the system. After 24hrs, this dark green solution is purified by centrifuge or dialysis to get well-dispersed polyaniline nanofiber dispersion.

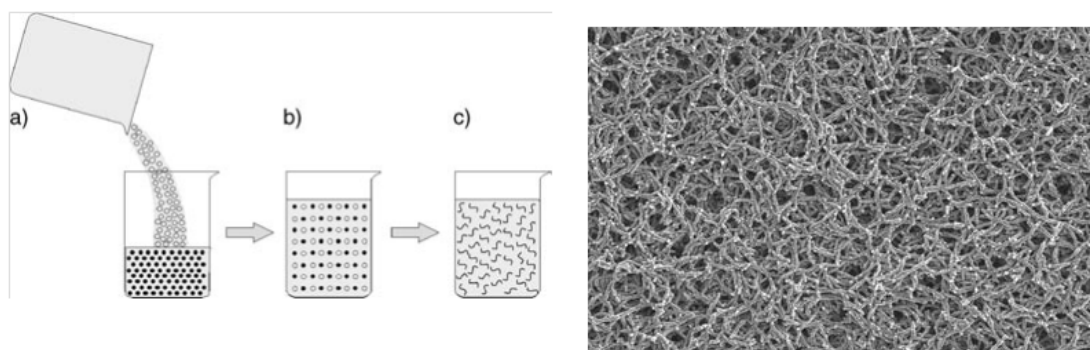


Figure 1.6 Synthesis of polyaniline in a rapidly mixed reaction a) The oxidant (open circles) dopant solution is quickly added into the aniline (solid circles) dopant solution and mixed. b) A homogenous solution is obtained where all the aniline and oxidant molecules are evenly distributed, thus leading to fast polymerization across the entire solution. c) Since all the reactants are consumed in the formation of nanofibers, secondary growth is suppressed. The right picture shows the nanofiber structure under SEM. Picture is published in *Angew. Chem.* 2004, 116, 5941.

The prepared polyaniline nanofibers dispersion is charge stabilized. When the monomer and oxidant are rapidly mixed, aniline and oxidant molecules are evenly distributed leading to a fast polymerization throughout the solution. This consumes all the available reactants in a short time and suppresses the second growth of polyaniline, which results in the granular, insoluble particles just like in the conventional synthesis. Different inorganic acids all result in nanofiber dispersion, with only diameter difference. Thus true pristine polyaniline dispersion can be made with all kinds of inorganic acids as dopants. Another big advantage is the nanofibular structure. Although the fiber-like structure make it not possible to cast a dense, durable film out of the solution, the high surface area between polymer and environment make it an ideal conducting polymer for sensor application.

With the use of aniline dimer and other aniline oligomers, nanofibers of polyaniline derivatives can also be successfully made as a stable aqueous dispersion. The low oxidation potential of these oligomers can speed up the otherwise slow polymerization and suppress the secondary growth of granular structures.[21] This method can be even applied to other conducting polymers like polypyrrole and polythiophene to synthesize template-free nanofibers of these polymers.[22]

#### **1.4 Polyaniline Derivatives**

As mentioned before, polyaniline can be chemically tailored by various methods to achieve the desired chemical and physical properties. Usually these polymer derivatives have better processability and other unique functionality but lower conductivity. Since not all the applications require the high conductivity in the range of 10-1000 S/cm, conductivity between  $10^{-1}$  and  $10^{-4}$  S/cm is still reasonable for a wide potential applications.

##### *Polymerization and Copolymerization of Aniline Derivatives*

Polymerization of aniline derivatives is the simplest way to make polyaniline derivatives. Both phenyl-substituted and N-substituted aniline can be polymerized through electrochemical or oxidative chemical polymerization. Sulfonated aniline can be polymerized to prepare water soluble self-doped polyaniline.[15-17] There are also many choices to increase the solubility of polymer in organic solvents, such as the use of 2-alkylaniline, N-alkylaniline, o-alkoxyaniline.[23, 24] Aniline derivatives can also be used to introduce a second active functional groups onto the polymer chain. For example, methacrylamide functional group can be attached onto N-phenylethylenediamine. This

new monomer was shown to possess orthogonal polymerization behavior to produce conjugated polyaniline suitable for a wide range of applications.[25]

Although these functional groups usually introduce conjugation defects and lower the conductivity, sometimes this can be overcome by secondary doping effect. Poly(o-toluidine) doped with d,l-camphorsulfonic acid in chloroform has a conductivity of 2S/cm.[13, 14] Copolymerization with aniline can also increase the conductivity at the cost of the potential processability.

#### *Post-modification of Polyaniline*

Because of the steric effect of the side group, polymerization of aniline monomers is always prepared in low molecular weight. To overcome this limitation, the substitution can be carried out by N-alkylation of polyaniline.[26] Either the emeraldine state or the fully reduced leucoemeraldine polyaniline can be used, but the leucoemeraldine polyaniline is preferred in some studies to maximize the substitution degree and minimize the side reactions. In a typical reaction, polyaniline is first dissolved in a strong base like dimethyl ion solution to deprotonate the amine group. Alkyl or other groups can be grafted onto the anionic polymer chain through nucleophilic substitution. A long alkyl group modified polymer shows good solubility in less polar solvent such as chloroform and toluene.[26]

### **1.5 Applications**

Discovered for more than 150 years, polyaniline is one of the most useful conducting polymers in a variety of application areas due to its ease of synthesis, simple yet rich

chemistries and environmental stability. With the help of nanotechnology, polyaniline can offer new properties compared the conventional dense counterpart. Our group first invented a general and facile route to synthesize water dispersible nanofibers of polyaniline and its derivatives for many applications.

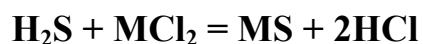
#### *Stable Dispersion for Coating*

Conventional polyaniline is insoluble in water at all like most other unfunctionalized conjugated conducting polymers. Although surfactants can stabilize the polymer, the conductivity usually sacrifices greatly. This processability problem also limits the application of other beautiful nanostructured polyaniline. Thus our dispersible, template-free polyaniline nanofibers solved this big problem and extend the application of nanostructured polyaniline in many ways. The solution can now be applied on all kinds of surface by common solution processing like spincoating, dipcoating, spraycoating and dropcasting. The dispersion can also mix with other noncharged, water-soluble polymers or small molecules to obtain a composite. The mechanical quality is of course not as strong as the dense polyaniline film, but the unique nanostructure makes it suitable as a sensor, supercapacitors and other applications where high surface area is required.

#### *Nanofiber-based Chemical Sensors*

The doping or dedoping process can change the conductivity of polyaniline over ten orders of magnitude. Thus polyaniline is a very sensitive material to many acid/base vapors. The porous nanofiber structure increases the interfacial contact between the polymer and the environment and enables chemical vapor diffuse into the entire

polyaniline film rapidly.[27] Compared to conventional dense films, this nanofiber-based chemiresistor shows much less response time and much higher sensitivity toward common strong acid and base vapors (such as HCl and NH<sub>3</sub>). The sensitivity is also thickness independent, which makes the device fabrication very simple. Besides this doping/dedoping mechanism, the nanofiber-based polyaniline sensors also perform better when exposed to reduction (by N<sub>2</sub>H<sub>4</sub>), swelling (by CHCl<sub>3</sub>) and the change of polymer conformation (by methanol). With the help of simple chemistry, polyaniline nanofibers can also detect weak acid and base. A polyaniline nanofiber film mixed with CuCl<sub>2</sub> can be used to detect H<sub>2</sub>S [28] because HCl is generated as a by-product::



Polyaniline derivatives bearing active functional groups can even be used to detect more chemicals. Poly(anilineboronic acid) can detect D-glucose based the chemistry of boronic acid. The formation of sugar diol-boronic acid complex can change the electrochemical potential of the polymer. A concentration as low as 5mM can be detected using this simple method.[29]

#### *Flash Welding [30]*

Exposed to strong light such as camera flash, polyaniline nanofibers will melt to a smooth, insulating film. Unlike conventional polyaniline films, each nanofiber has very limited contact with other fibers. Thus the heat converted from light energy cannot dissipate to surrounding polyaniline efficiently. The temperature of the single fiber rises rapidly and welds the nanofibers to obtain a continuous film. SEM image shows that only the top layer of the film exposed to light is welded while the bottom layer remains the

fiber structure. This asymmetric film can be used as chemical induced actuators. As the film doped with acid, the nanofiber layer of the film expands due to the electrostatic repulsion, resulting in the bending of the film. (Figure 1.7)

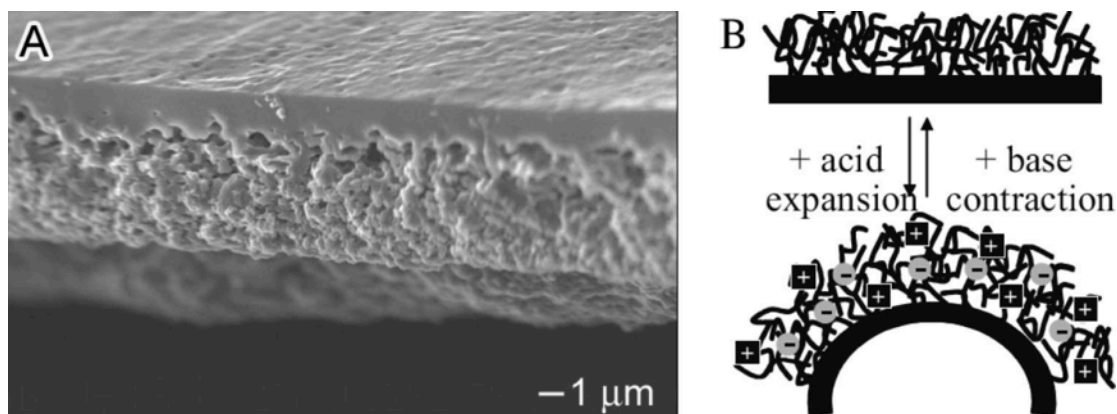


Figure 1.7 (A) An SEM image of a flash welded film with an asymmetric cross section (B) The actuation of the as-formed asymmetric film upon exposure to an acid or base. Picture is published in *Acc. Chem. Res.*, 2009, 42, 135.

### *Polyaniline Nanofiber/metal Nanoparticle Composites*

Because of the porous structure and large surface area, Polyaniline nanofibers can be used as scaffold for inorganic nanoparticles. Treated with metal salts, polyaniline fibers function as both reducing agent and stabilizer. This eliminates the step of further reduction. The resulting composites will still keep the nanostructure and the dispersibility in water. A composite of polyaniline/palladium nanoparticles reported by our group [31] is tested as a new semi-heterogeneous catalyst in water. The supported palladium particles are active catalysts for Suzuki coupling between aryl chlorides and phenylboronic acid. The final product can be extracted into organic phase and then separated.



## **1.6 Conclusions**

As a very inexpensive conducting polymer, polyaniline has many attractive chemical and physical properties. With decades' study of this material, researchers fully investigated the mechanism of polymerization, the possible chemistry on the polymer chain and the physical properties of polyaniline. Now this thermal stable conducting polymer can be dispersed in many organic solvents as well as water. The conductivity can be tuned to as high as 400S/cm. Functionalized polyaniline are also synthesized in different ways to meet the specific requirement. The processable nanofiber dispersion in water expands the application greatly. With the current knowledge, polyaniline has a very good chance to replace the current material in many applications.

## 1.7 References

1. J. L. Bredas and G. B. Street, *Acc. Chem. Res.* **1985**, 18, 309.
2. Prasanna Chandrasekhar, *Conducting Polymers, Fundamentals and Applications a Practical Approach*, Kluwer Academic Publishers, **1999**.
3. H. Lethaby, *J. Chem. Soc.* **1862**, 15, 161.
4. Vaman G. Kulkarni, Larry D. Campbell and William R. Mathew, *Synthetic Metals* **1989**, 321.
5. Yen Wei, Guang- Way Jaag, Chi-Cheung Chan, Kesyin F. Hsueh, Ramakrishnan Hariharan, Sandeep A. Patel, and Charles K. Whitecar, *J. Phys. Chem.* **1990**, 94, 7717.
6. P.N. Adams, P.J. Laughlin, A.P. Monkman, *Synthetic Metals* **1996**, 76, 157.
7. L. Dennany, P. C. Innis, S. T. McGovern, G. G. Wallacea and Robert J. Forsterb, *Phys. Chem. Chem. Phys.* **2011**, 13, 3303.
8. A.G. MacDiarmid, S.K. Manohar, J.G. Masters, Y. Sun, H. Weiss, *Synthetic Metals* **1991**, 41, 621.
9. Yen Wei , Kesyin F. Hsueh , Guang Way Jang, *Macromolecules* **1994**, 27, 518.
10. K. R. Cromack, M. E. Jozefowicz, J. M. Ginder, A. J. Epstein, R. P. McCall, G. Du, J. M. Leng, K. Kim, C. Li, and Z. H. Wane, *Macromolecules* **1991**, 24, 4157.
11. A.G. Macdiarmid, Y. Min, J.M. Wiesinger, E.J. Oh, E.M. Scherr and A.J. Epstein, *Synthetic Metals* **1993**, 55, 753.
12. Yong Cao, Paul Smith and Alan J. Heeger, *Synthetic Metals* **1992**, 48, 91.
13. A.G. MacDiarmid, Arthur J. Epstein, *Synthetic Metals* **1994**, 65, 103.
14. A.G. MacDiarmid, Arthur J. Epstein, *Synthetic Metals* **1995**, 69, 85.
15. Jiang Yue, Arthur J. Epstein, *J. Am. Chem. Soc.* **1990**, 112, 2801.
16. My T. Nguyen, Paul Kasai, James L. Miller, and Arthur F. Diaz, *Macromolecules* **1994**, 27, 3625.
17. Fatemeh Masdarolomoor, Peter C. Innis, Syed Ashraf, Richard B. Kaner and Gordon G. Wallace, *Macromol. Rapid Commun.* **2006**, 27, 1995.

18. Moon Gyu Han, Seok Ki Cho, Seong Geun Oh, Seung Soon Im, *Synthetic Metals* **2002**, 126, 53.
19. Jiaying Huang, Shabnam Virji, Bruce H. Weiller and Richard B. Kaner, *J. Am. Chem. Soc.* **2003**, 125, 314.
20. Jiaying Huang and Richard B. Kaner, *Angew. Chem.* **2004**, 116, 5941.
21. Henry D. Tran and Richard B. Kaner, *Chem. Commun.* **2006**, 3915.
22. Henry D. Tran, Yue Wang, Julio M. D'Arcy, and Richard B. Kaner, *ACSNANO*, **2008**, 2, 1841.
23. Akira Watanabe, Kunio Mori, Atsushi Iwabuchi, Yasunori Iwasaki, and Yoshiro Nakamura, *Macromolecules* **1989**, 22, 3521.
24. David MacInnes, JR. and B. Lionel Funt, *Synthetic Metals* **1988**, 25, 235.
25. Dhana Lakshmi, Micael J. Whitcombe, Frank Davis, Iva Chianella, Elena V. Piletska, Antonio Guerreiro, Sreenath Subrahmanyam, Paula S. Brito, Steven A. Fowler and Sergey A. Piletsky, *Chem. Commun.* **2009**, 2759.
26. Wen-Yue Zheng and Kalle Levon, Jukka Laakso and Jan-Eric Osterholm, *Macromolecules* **1994**, 27, 7754.
27. Shabnam Virji, Jiaying Huang, Richard B. Kaner and Bruce H. Weiller, *Nano Lett.* **2004**, 4, 591.
28. Shabnam Virji, Jesse D. Fowler, Christina O. Baker, Jiaying Huang, Richard B. Kaner, and Bruce H. Weiller, *Small* **2005**, 1, 624 .
29. Eiichi Shoji and Michael S. Freund, *J. Am. Chem. Soc.* **2001**, 123, 3383.
30. Dan Li, Jiaying Huang and Richard B. Kaner, *Acc. Chem. Res.* **2009**, 42, 135.
31. Benjamin J. Gallon, Robert W. Kojima, Richard B. Kaner, and Paula L. Diaconescu, *Angew. Chem.* **2007**, 46, 7251.

## **Chapter 2 Dispersions of Polyaniline/Carbon Nanotubes in Organic Solvents as Conductive Fillers for Polyurethane**

### **2.1 Introduction**

Solution processable polyaniline in water or organic solvents has been synthesized in the past two decades with moderate or high conductivity. One interesting application is to use these well-dispersed/dissolved polymers as lightweight conducting fillers in other common polymer matrices, such as polyurethane and epoxy resin. The only requirement is to find a solvent that can dissolve both polyaniline and the polymer matrix. Cao et al. reported that a 2% loading of polyaniline/camphorsulfonic acid (CSA) in poly (methyl methacrylate) (PMMA) polyblends can reach a conductivity of 1 S/cm if m-cresol is used as the solvent.[1] Although this is exciting, the high toxicity and boiling point of m-cresol limits the application of this system. A relatively benign polyaniline/dodecylbenzenesulfonic acid (DBSA) solution in toluene is also measured with a percolation ten times higher than the former one (what is the former one? Please spell this out). The percolation threshold depends on how favorable the filler forms a conductive route through a self-assembly process. The soft nature of polyaniline may also lower the mechanical strength of the composite at a high percentage loading.

An alternative way to solve the problem is to use dispersible carbon materials such as graphene and/or carbon nanotubes, as conducting fillers. These carbon materials are lightweight, mechanically strong and highly conductive. There are three major ways to disperse graphene or carbon nanotubes into a polymer matrix: physical blending [2-4], chemical modification [5-9] and surfactant-assisted dispersion [10-14]. Each of these methods has its advantages and disadvantages. Physical blending such as powerful

sonication avoids the use of any surfactant, but the quality of the dispersion is poor. Precipitates may form as soon as the sonication stops. Chemical modification can produce stable dispersions or solutions by introducing proper functional groups, but the functionalization often destroys the degree of conjugation of the carbon backbone and hence, lowers the conductivity greatly. Surfactants can produce stable, pristine carbon solutions, but these surfactants will prevent electron transfer from one carbon nanotube (or graphene sheet) to another one.

Thus, a smart way is to disperse carbon nanotubes or graphene into a conducting polymer, and then load the conducting polymer into the polymer blend. The conjugated conducting polymers have strong  $\pi$ - $\pi$  interactions with carbon materials. A stable dispersion of conducting polymer/carbon material can be obtained as long as the conducting polymer is well dispersed in the solvent. Compared to other methods, the carbon materials remain pristine and do not sacrifice conductivity or strength; the conductive nature makes these conducting polymers far superior to other surfactants in terms of electron transfer throughout the whole composite. Because of these unique advantages, many conducting polymer/carbon dispersions have been studied in recent years. For example, an aqueous solution of PEDOT: PSS can stabilize up to 200% loading of multi-wall carbon nanotubes for several weeks.[15] At this loading, the sheet resistance decreases up to 500 times. Interestingly, the PEDOT: PSS solution can even disperse graphite nanoplatelets well in water [16], which can be viewed as tens of layers of graphene of micron size. Studies on polyaniline reveal strong interactions between polymer and carbon nanotubes if the polymerization takes place in the presence of carbon

nanotubes. A sulfonation process can stabilize these composites in aqueous solution due to the presence of water-soluble sulfonic acid groups. [17] Our group has also successfully prepared aqueous dispersible carbon nanotube/polyaniline nanofibers [18] through a rapidly mixing reaction as discussed in Chapter 1.3. This core/shell nanofibrillar structure can be used to create much faster gas sensors compared to polyaniline nanofibers alone because of the greatly improved conductivity. A polyaniline stabilized graphene aqueous solution can also be prepared if polystyrenesulfonic acid is used as a dopant and co-surfactant.[19] Recently, a solution of polyaniline/single wall carbon nanotubes (SWCNTs) in a common organic solvent was synthesized by a phase transfer method in the presence of excess ionic surfactants.[20] This expands the applications of the composite to many oil-based polymer matrices like solvent-based polyurethane and epoxy resins.

Here we report a simple method to synthesize a solution of polyaniline and single wall carbon nanotube composites in common organic solvents. Under the condition of mild sonication, SWCNTs can disperse homogeneously into polyaniline/DBSA solutions in common organic solvents like chloroform, toluene and xylene. Up to 100% carbon nanotubes (based on the weight of the polyaniline emeraldine base) can disperse well in polyaniline without any visible particles. (Figure 2.1) The conductivity of a polyaniline/DBSA/SWCNT composite increases more than 100 times at a high loading level. It can also be used as effective conductive filler in a commercially available two-part polyurethane system. The polyurethane incorporated SWCNT shows much higher conductivity compared to one with only polyaniline.

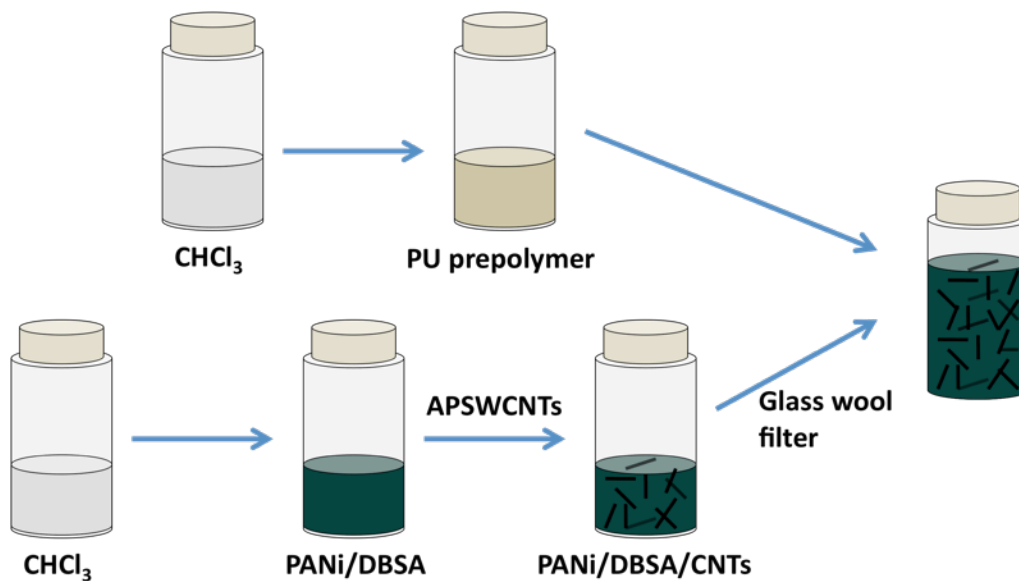


Figure 2.1 Process to prepare polyaniline/DBSA/SWCNT composite in an organic solvent. The final composite is stable with no visible particles.

## 2.2 Experiment section

### *Materials and Characterization*

All materials were used as received without further purification. Aniline, ammonium peroxydisulfate were purchased from Sigma Aldrich. DBSA was received from MP Biomedicals LLC. Concentrated ammonium hydroxide was obtained from BDH. Concentrated HCl was purchased from Fisher Scientific. AP-SWCNT (As prepared single-wall carbon nanotubes) were obtained from Carbon Solutions Inc. Forsch 80A Clear Cast two parts polyurethane systems was obtained from McMaster-Carr. Field emission scanning electron microscopy (SEM, JEOL JSM-6700) was used to observe the morphologies of PANi/DBSA/SWCNT samples. UV-vis spectroscopy was carried out on an HP 8453 spectrometer. Sheet resistance is measured by a two-probe multi-meter.

### *Synthesis of Polyaniline Nanofibers in Emeraldine Base Form*

Polyaniline was synthesized by a rapid mixing method.[21] In a typical synthesis, 29.2 ml of aniline is dissolved in 1 L of 1 M HCl and 18.25 grams of ammonium persulfate is dissolved in another 1 L of 1 M HCl. The two solutions are combined rapidly and shaken for 15 s to well mix monomer and oxidant. The mixture is allowed to sit still for 24 hours. The polyaniline nanofibers dispersion is then filtered and washed with another 2 L of distilled water to remove any oligomers and excess monomer. The green precipitate on the filter paper is suspended in excess 0.1 M ammonium hydroxide (NH<sub>4</sub>OH) solution for at least one hour to fully deprotonate the polyaniline. The blue polyaniline emeraldine base is filtered again and washed with another 2 L of distilled water to remove the generated ions and excess NH<sub>4</sub>OH. The final product on filter paper is dried in vacuum oven at 40 °C overnight. The yield is around 20%. The product is then ground into a fine powder for the next step.

### *Synthesis of Polyaniline/DBSA Solution in Organic Solvents*

The counter-ion induced polyaniline solution is prepared according to a reported procedure.[1] To make a chloroform solution, 1 gram of synthesized polyaniline powder and 3.6 grams of DBSA (molar ratio between aniline and DBSA is 1: 1) are mixed in 100 ml of chloroform. The mixture is sonicated overnight. The green polyaniline/DBSA solution is then filtered through glass wool to remove any insoluble solids. The solution is diluted to 2% for the next step. For a toluene solution, half the amount of polyaniline and DBSA is used without further dilution.



### *Synthesis of Polyaniline/DBSA/SWCNT Composite Solution*

Different amounts of AP-SWCNT are added to 10 ml of a polyaniline DBSA solution. The mixture is sonicated for 6 hours. The final solution is filtered through glass wool to remove any insoluble solids. The loading percentage is based on the weight of the polyaniline emeraldine base.

### *Synthesis of Conductive Polyurethane Composites*

1 g of polyol and 900 mg of isocyanate are mixed in chloroform to obtain a 20% solution. The solution is stirred for 1 hour to polymerize. An appropriate amount of polyaniline/DBSA/SWCNT solution is then added to achieve a desired loading of conducting filler. The solution is then spray-coated onto a 1 inch by 1 inch glass slide and cured for 24 hours at 50 °C. Scheme 2.1 shows the process of preparing a conductive polyurethane film.

## **2.3 Results and Discussion**

The conductivity of polyaniline in organic solvents is mainly determined by a secondary doping effect [22, 23], as is discussed in Chapter 1.3. Concerning conductivity, CSA doped polyaniline in m-cresol will be the best system to load carbon nanotubes. However, the highly toxic m-cresol with a high boiling point greatly limits application to prepare polyurethane composites. Thus, chloroform and toluene were chosen instead with DBSA as the dopant. Previous studies have shown that a 1:1 molar ratio between aniline units and dopants is required to maximize the conductivity and solubility [22, 23].

Carbon nanotubes themselves are not soluble at all in chloroform or toluene even in the presence of DBSA. (Figure 2.2a) So clearly the strong interactions with polyaniline

stabilize the carbon nanotubes enabling them to disperse into the solution. AP-SWCNTs are used in the experiments without any further treatment. Although these ‘dirty’ tubes have about 30% metal catalyst and some amorphous carbon impurities, they cost only 25 dollars per gram while P2-SWCNT (purified carbon nanotubes without functional groups on their surfaces) cost 400 dollars per gram. The PANI/DBSA solution in toluene tends to form a gel even without carbon nanotubes at high concentrations. Thus, most experiments are based on chloroform solutions. However, if toluene is a desired solvent for the polyurethane system, the polyaniline-carbon nanotube solution can be synthesized and used as long as it is freshly made.

Up to 100% SWCNT (which is 5 mg/ml for a 2% polyaniline/DBSA solution) can be dispersed in chloroform to form a homogeneous solution without any visible particles. (Figure 2.2a) However, the solution with 100% SWCNT is much more viscous than the 25% one. When the loading percentage is increased to 200%, the mixture turns into an organogel after sonication. (Figure 2.2b) A similar phenomenon is noticed when a 1% graphite oxide aqueous solution is added into 2% PEDOT: PSS solution under sonication.[24] It is believed that the interaction between polymer and carbon is responsible for the gelation because carbon nanotubes do not gel in the presence of only DBSA. The increased viscosity also indicates that carbon nanotubes are not fully debundled, and this is confirmed by a simple dilution experiment. (Figure 2.2c) Solutions with 100% SWCNT and 25% SWCNT are diluted over ten times in chloroform. The 25% one is still clear without any visible precipitates; however, the 100% percent “solution” exhibits floating black agglomerates in 3-5 minutes. At low concentrations, polyaniline is

not able to hold these extra, not fully wrapped carbon nanotubes in solution. Thus, no more than 50% loaded solutions are used for polyurethane film preparation.

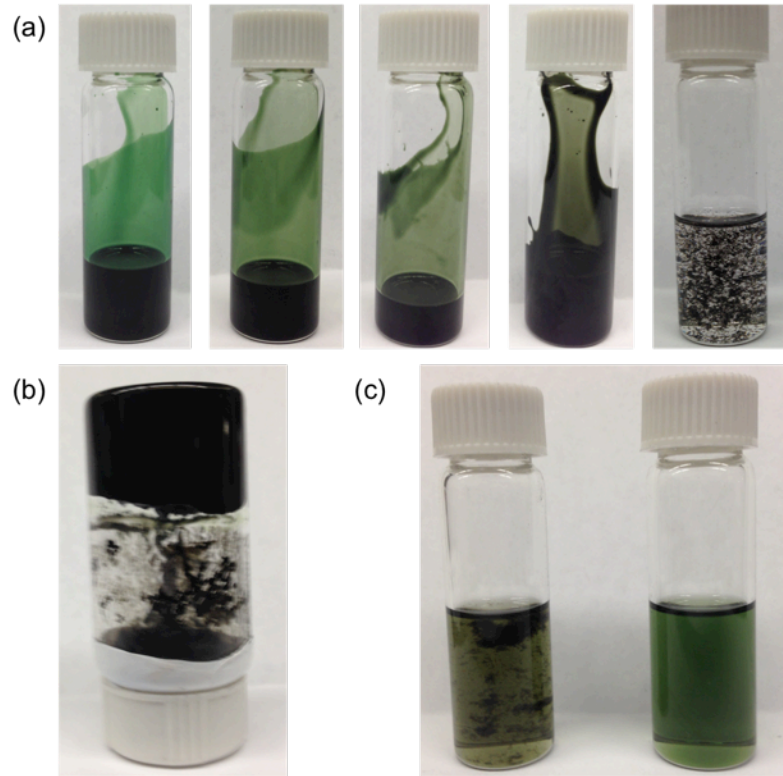


Figure 2.2 (a) From left to right: solutions of polyaniline/DBSA with 0%, 25%, 50% and 100% carbon nanotube loadings in chloroform. The solutions are clear without any visible particles. The rightmost one is carbon nanotubes in DBSA only (without polyaniline). (b) Gel forms at over 200% carbon loading. (c) After dilution, the carbon nanotubes at 100% loading precipitates (left), while the 25% loading solution (right) is still clear and stable.

Polyaniline/DBSA/SWCNT solutions are spin-coated on 1 inch by 1 inch glass slides to obtain transparent conductive films. (Figure 2.3a) The sheet resistance increases more than 100 times with 100% SWCNT loading (to 1.1 Kohm) compared to the pure polyaniline solution (160 Kohm). The color of the films darkens when the carbon loading

increases because of the light absorbance of carbon nanotubes. The SEM images reveal that carbon nanotubes are well connected in the polyaniline matrix. (Figure 2.3c) They act like nanobridges throughout the film and enhance the conductivity greatly. The bright nanoparticles in the images are likely metal catalyst particles left in the AP-SWCNT. The incorporated carbon nanotubes also increase the mechanical strength of the composite. Both polyaniline/DBSA and polyaniline/DBSA/SWCNT solutions were drop-cast on glass slides to obtain thick films. When rinsed with water, the film with the SWCNTs still keeps its shape, while the other one breaks into pieces due to its poor strength. The carbon nanotubes in this case function as a strong scaffold that holds the film together. (Figure 2.3d)

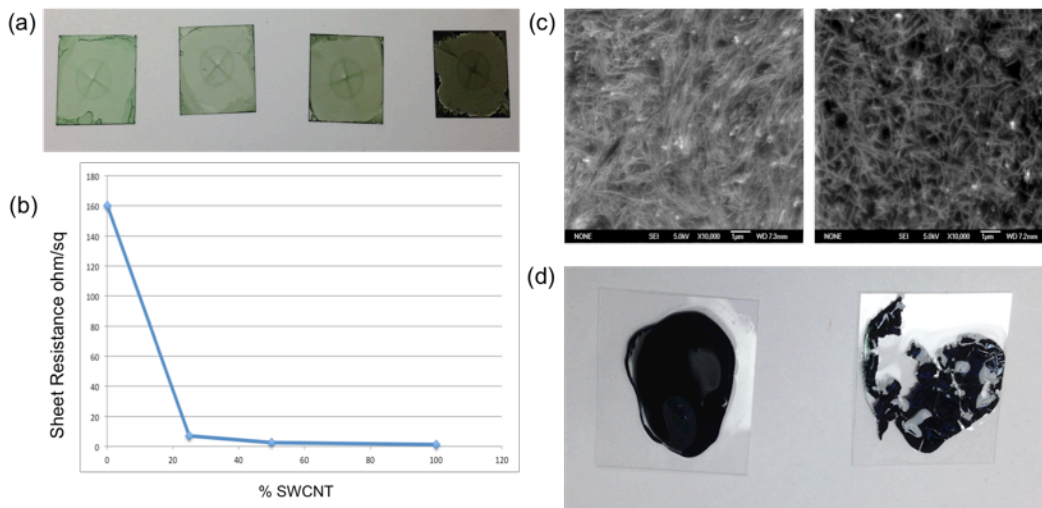


Figure 2.3 (a) From left to right: spin-coated thin films from polyaniline/DBSA solution with 0%, 25%, 50% and 100% SWCNT loading. (b) Sheet resistance of spin-coated films with different SWCNT loading. (c) SEM images of polyaniline/DBSA/SWCNT composites in chloroform (left) and toluene (right). (d) Polyaniline/DBSA solution without SWCNT (right) and with 25% SWCNT (left) drop-cast to obtain thick films. After rinsing with water, the film without the SWCNTs breaks into pieces due to its poor mechanical properties.

The polyaniline/DBSA/SWCNT composite can be introduced into a polyurethane matrix as a conducting filler to prepare conductive polyurethane composites. The only requirement is that the polymer matrix is also compatible with the solvent. Toluene and chloroform are sufficient for most non-polar or moderate polar matrices. In these experiments different weight amounts of conducting fillers are loaded into polyurethane (the percentage is based on the weight of the polyurethane). The presence of carbon nanotubes cannot only increase the conductivity, but the mechanical properties as well.

Table 2.1 shows the sheet resistance of spray-coatings at different loading percentages. It is not surprising that the conductivity is roughly proportional to the amount of conducting fillers and the percentage of carbon nanotubes in the conducting fillers. However, the thickness of each film, the air pressure and the amount of polyurethane composite are not well controlled under the experimental conditions. Thus, the uniformity and quality are different from sample to sample. Nevertheless, the results confirm the importance of carbon nanotubes in the composites. The polyurethane composite films are mechanically tough at least to a simple test, i.e. they withstand peeling with Scotch tape.

Table 2.1 Sheet Resistances of Polyurethane Composite Films Cast by Spray-Coating

	Sheet Resistance with Different Percentage Loading of Polyaniline/DBSA/SWCNT				
Percentage of SWCNT in PANI/DBSA	5%	10%	20%	30%	40%
0%	-	12 Mohm	3.2 Mohm	2.4 Mohm	250 Kohm

25%	14 Mohm	1.2 Mohm	40 Kohm	52 Kohm	14 Kohm
50%	13 Mohm	340 Kohm	17 Kohm	14 Kohm	5 Kohm

SEM images provide a close look at the surfaces of these polyurethane films with carbon nanotubes. As is shown in Figure 2.4, carbon nanotubes are dispersed everywhere in the polymer matrix. They are connected throughout the whole film to form conductive pathways. There are many milky circles on the surface of the composite film, which are bundles of aggregated carbon nanotubes. These aggregated SWCNTs are partially aligned, and thus, the aggregation is probably caused by solvent evaporation.

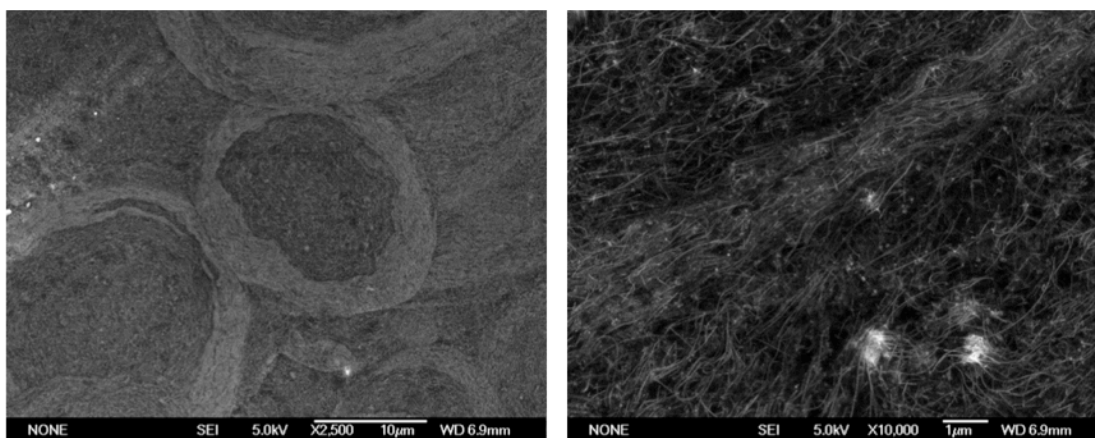


Figure 2.4 Left: a low magnitude picture of polyurethane composite. Carbon nanotubes are connected to form conductive pathways. Right: A zoomed-in picture of milky circles in the left picture. These white bands are composed of bundles of partially aligned carbon nanotubes. They are probably caused by solvent evaporation.

These conducting polyurethanes can be used as transparent coatings. (Figure 2.5a) Polyurethane composites incorporated with different amounts of polyaniline/DBSA/0.25SWCNT were spray-coated onto glass slides to obtain thin films.

Although the films have a light green color, we can easily recognize all seven colors of the rainbow pattern beneath the films. The transmittance measurement of the film with 30% conductive filler reveals a transmittance over the visible region of around 80 percent. (Figure 2b) The highest region of transparency for these films occurs between around 480 to 620 nm, indicating that the material should take on the green color associated with doped polyaniline.

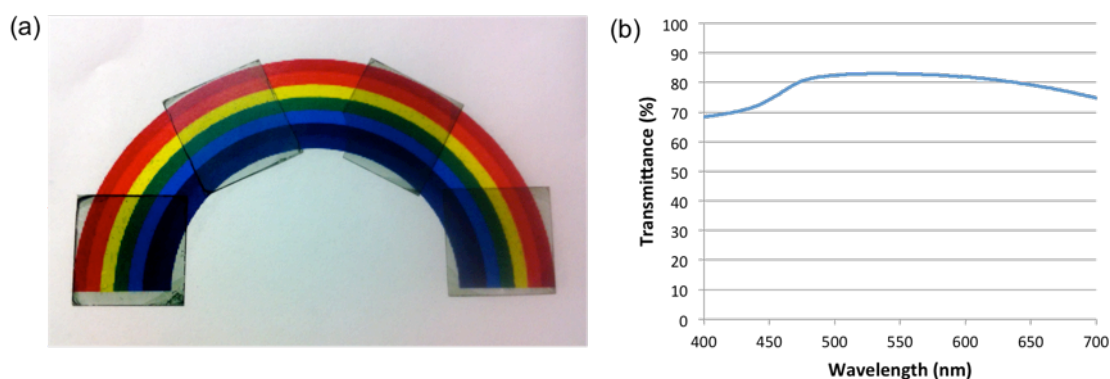


Figure 2.5 (a) Thin films of polyurethane films incorporated with polyaniline/DBSA/0.5SWCNT. The loading percentages from left to right are 10%, 20%, 30% and 40%. (b) Visible transmittance spectrum of 30% loaded film.

## 2.4 Conclusions

SWCNTs can be incorporated into a polyaniline/DBSA solution in common organic solvents to obtain a stable dispersion by mild sonication. Up to 100% carbon nanotubes can be loaded into polyaniline without any visible precipitates. This polyaniline/DBSA/SWCNT solution can be spin-coated into transparent thin films on substrates with potential applications as transparent electrodes. Moreover, it can also be combined with organic solvent-based polyurethane and spray-coated to obtain a conductive polyurethane composite film. The carbon nanotubes increase the conductivity

of the composite greatly by forming conductive pathways throughout the film. This composite can be applied to many substrates to form transparent conductive coatings.



## 2.5 References

1. Yong Cao, Paul Smith and Alan J. Heeger, *Synthetic Metals*, **1992**, 48, 91.
2. M. B. Bryning, M. F. Islam, J. M. Kikkawa, A. C. Yodth, *Adv. Mater.* **2005**, 17, 1186.
3. J. C. Kearns, R. L. Shambaugh, *J. Appl. Polym. Sci.* **2002**, 86, 2079.
4. J. K. W. Sandler, J. E. Kirk, I. A. Kinloch, M. S. P. Shaffer, A. H. Windle, *Polymer* **2003**, 44, 5893.
5. E. T. Mickelson, C. B. Huffman, A. G. Rinzler, R. E. Smalley, R. H. Hauge, J. L. Margrave, *Chem. Phys. Lett.* **1998**, 296, 188.
6. J. L. Bahr, J. M. Tour, *Chem. Mater.* **2001**, 13, 3823.
7. V.A.Davis,L.M.Ericson,A.N.G.Parra-Vasquez,H.Fan,Y.Wang, V. Prieto, J. A. Longoria, S. Ramesh, R. K. Saini, C. Kittrell, W. E. Billups, W. W. Adams, R. H. Hauge, R. E. Smalley, M. Pasquali, *Macromolecules* **2004**, 37, 154.
8. F. Liang, A. K. Sadana, A. Peera, J. Chattopadhyay, Z. Gu, R. H. Hauge, W. E. Billups, *Nano Lett.* **2004**, 4, 1257.
9. Y. Ying, R. K. Saini, F. Liang, A. K. Sadana, W. E. Billups, *Org. Lett.* **2003**, 5, 1471.
10. M. S. Strano, V. C. Moore, M. K. Miller, M. J. Allen, E. H. Haroz, C. Kittrel, R. H. Hauge, R. E. Smalley, *J. Nanosci. Nanotechnol.* **2003**, 3, 81.
11. M. F. Islam, E. Rojas, D. M. Bergey, A. T. Johnson, A. G. Yodh, *Nano Lett.* **2003**, 3, 269.
12. R. Bandhyopadhyaya, E. Nativ-Roth, O. Regev, R. Yerushalmi- Rozen, *Nano Lett.* **2002**, 2, 25.
13. R. Shvartzman-Cohen, Y. Levi-Kalishman, E. Nativ-Roth, R. Yerushalmi-Rozen, *Langmuir* **2004**, 20, 6085.
14. J. C. Grunlan, L. Liu, Y. S. Kim, *Nano Lett.* **2006**, 6, 911.
15. Dong-Jin Yun, KiPyo Hong, Se hyun Kim, Won-Min Yun, Jae-young Jang, Woo-Sung Kwon, Chan-Eon Park, and Shi-Woo Rhee, *Applied Materials & Interfaces* 2001, 3, 43.
16. Jue Lu, Inhwan Do, Hiroyuki Fukushima, Ilsoon Lee, and Lawrence T. Drzal, *Journal of Nanomaterials*, **2010**, Article ID 186486.
17. Hui Zhang, Hong X. Li, and Hui M. Cheng, *J. Phys. Chem. B* **2006**, 110, 9095.

18. Yaozu Liao, Chen Zhang, Ya Zhang, Veronica Strong, Jianshi Tang, Xin-Gui Li, Kourosh Kalantar-zadeh, Eric M. V. Hoek, Kang L. Wang and Richard B. Kaner, *Nano Lett.* **2011**, 11, 954.
19. Jing Luo, Sisi Jiang, Yong Wu, Meiling Chen, Xiaoya Liu, *J. Polym. Sci. A Polym. Chem.* **2012**, 50, 4888.
20. Sainath G. Vaidyaan, Sanjay Rastogia,b, Aránzazu Aguirre, *Synthetic Metals* **2010**, 160, 134.
21. Jiaying Huang and Richard B. Kaner, *Angew. Chem.* **2004**, 116, 5941.
22. A.G. MacDiarmid, Arthur J. Epstein, *Synthetic Metals* **1994**, 65, 103.
23. A.G. MacDiarmid, Arthur J. Epstein, *Synthetic Metals* **1995**, 69, 85.
24. Vincent C. Tung, Jaemyung Kim, Laura J. Cote, and Jiaying Huang, *J. Am. Chem. Soc.* **2011**, 133, 9262.

## **Chapter 3 A Novel Water-Soluble Synthetic Mussel Adhesive**

### **3.1 Introduction**

Adhesives play a very important role in our daily lives, although we may not even be aware of them. Envelopes, band-aids, baby diapers, wallpaper, furniture joints, floor tiles, etc.; all these common items use some kind of adhesives. High quality duct tape even helped save the Apollo 13 crew. The use of adhesive substances dates back to 4000 B.C.; however, most of the technology of adhesives has been developed during the past 100 years due to the development of plastics and elastomers.[1] The adhesives manufacturing market was over 11 billion dollars in 2011 in the United States, and market researchers forecast a turnover of almost 50 billion dollars for the global adhesives market by 2019.[2]

Currently, various synthetic adhesives dominate the market, such as epoxies, cyanoacrylates, hot melt adhesives and pressure sensitive tapes. Naturally produced adhesives in many biological systems have drawn more and more attention in recent years because of their superior strength and durability compared with man-made materials. For example, the spider silks made of adhesive proteins have high tensile strength, extensibility, and an energy-dissipative viscoelastic response that is not matched by synthetic polymers.[3] These naturally produced high quality adhesives inspire scientists to study their adhesive mechanism and to design various synthetic biomimetic adhesives that can be applied on a biological or non-biological surface.

Another natural adhesive from mussels is also receiving growing interest because it is incredibly strong and durable in an aqueous environment. Marine mussels can attach to a variety of solid surfaces in wave-swept seashores. The adhesion is applied through a holdfast structure called a byssus, i.e. a bundle of long silky threads tipped by adhesive plaques, which can attach mussels to hard surfaces (Figure 3.1a). More than ten proteins have been identified from the byssus.[4] Most of them present in the adhesive plaques such as Mytilus foot protein-3 (mfp-3) and mfp-5. However, some of these adhesive proteins are not limited to plaques. Mfp-1, for example, functions as a protective cuticle covering the exposed part of byssus (Figure 3.1b).

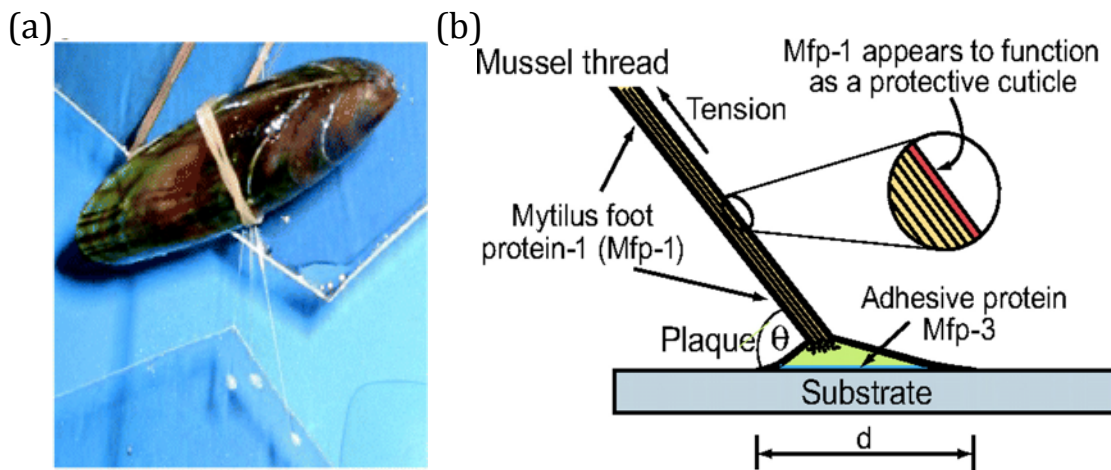


Figure 3.1 (a) Mussel is connected to a mica sheet using byssal threads. (b) Schematic drawing of a byssal thread attached to a substrate. Different mussel foot proteins are located at different places. The picture has been adapted from Reference 4.

Despite different locations, molecular weights and structures, all these adhesive proteins contain the post-translationally modified amino acid, 3, 4-dihydroxyphenyl-L-alanine (L-DOPA), which is the key component of mussel adhesion mechanism (Figure 3.2). The L-DOPA content ranges from a few percent to above 20%.[4,5] L-DOPA forms both

adhesive and cohesive bonds through its reduced and oxidized (L-DOPA quinone) states (Figure 3.2).[5] The adhesion refers to the interaction between the adhesive plaque and the environmental surface, whereas cohesion refers to the bulky elastic properties of the adhesive. The catechol group in reduced L-DOPA is capable of bonding strongly to hydrophilic surfaces through bidentate hydrogen bonding, or bond to metal oxide surfaces by chelation. The cohesion is vital to the strength of the bulk material. The reduced L-DOPA can form strong complexes with metal ions especially with iron, whereas the oxidized L-DOPA quinone is able to form intermolecular crosslinking, which can occur spontaneously in alkaline pH. Whereas too much L-DOPA quinone will cause interfacial failure; too much reduced L-DOPA will lead to cohesive failure. Mussels balance the redox chemistry of L-DOPA carefully to achieve the best plaque adhesion. Physical adhesion also plays a very important role in the mussel adhesive. Mfp-3 and mfp-5 in the plaques have very small molecular weights, which enable them to diffuse into the pores of the contact surface and then interlock. Mussels can adhere strongly to most natural and synthetic surfaces, both hydrophilic and hydrophobic, by electrostatic, hydrogen bonding,  $\pi$ - $\pi$  stacking, cation- $\pi$  and metal complexation.[6] Besides L-DOPA, these mussel adhesive proteins also contain excess cationic amino acids such as lysine and arginine.[7] These positively charged amines exhibit favorable electrostatic interactions with the negatively charged surfaces even under the sea.[8]

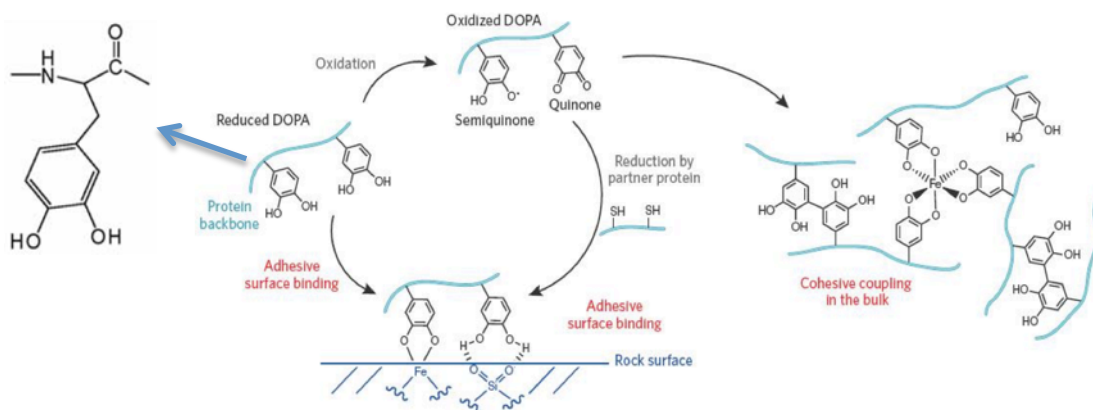


Figure 3.2 L-DOPA forms strong adhesive bonds by bidentate hydrogen bonding and metal/metal oxide coordination (left). L-DOPA that has been oxidized to L-DOPA quinone can be reduced by thiol-containing groups to form adhesive bonds (center). L-DOPA quinone can also participate in cohesive oxidative crosslinking and metal chelation to form the bulk material (right). The picture is adapted from Reference 5.

Obtaining mussel adhesive proteins can be difficult. For example, approximately 10,000 *M. edulis* mussels are needed to produce 1 g of Mfp-1 adhesive from byssal structures by extraction under acidic conditions.[9] Expression of these proteins can also be carried out in microbial hosts using recombinant DNA technology [10], but the large-scale generation is complicated and expensive. Because of these difficulties, synthesis of biomimetic mussel foot proteins has gained rapidly increasing investigation. The adhesive ability of mussel foot proteins or synthetic mussel adhesives are affected by many factors such as the percentage of L-DOPA, the molecular weight, the backbone properties and the affects of other functionalities. In fact, the exact role of L-DOPA and the mechanism of adhesion are still not fully understood. As a result, the as-prepared synthetic mussel adhesives may be not suitable for adhesion, but can be used for other interesting applications such as hydrogels, surface treatments, antifouling coatings and more. (a) Synthetic polypeptides with lysine and L-DOPA residues can adhere to steel,

aluminum, glass and various substrates via oxidative crosslinking.[11]

(b) L-DOPA-containing polyacrylates and related copolymers show strong adhesion under wet conditions. These kinds of polymers have potential applications as waterborne medical adhesives.[12-14]

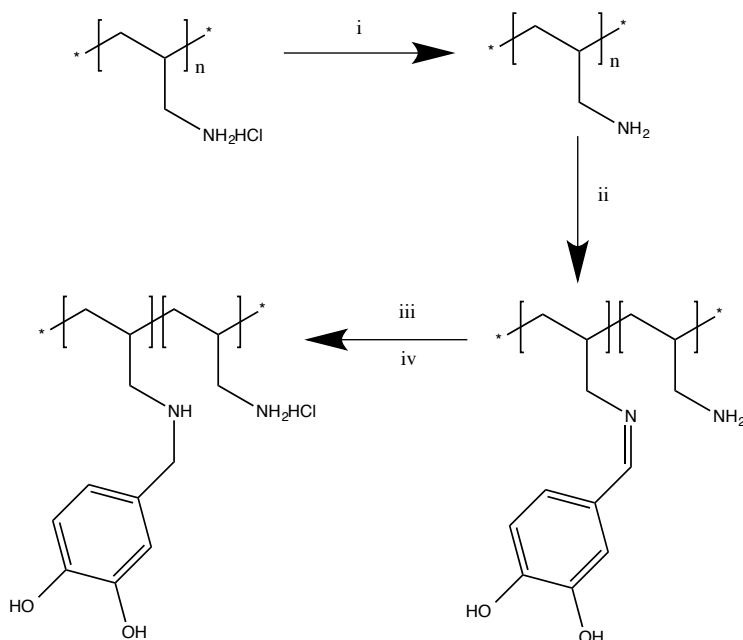
(c) L-DOPA terminated polyethylene glycols are synthesized by various methods with different functionalities. These catechol containing polymers tend to form hydrogels when cross-linked by oxidants or metal ions.[15] They are also suitable for anti-fouling coatings.[16-18]

(d) A thin film of polydopamine can be coated onto various substrates by self-polymerization of dopamine under alkaline condition with applications in medical science, water treatment and sensing.[19]

(e) Poly[(3,4-dihydroxystyrene)-co-styrene] and its derivatives can adhere two slides of glass, steel or aluminum together with strong adhesion even comparable to commercial superglue.[8, 20, 21] Interestingly, the polymer was first synthesized and studied almost 30 years ago [22], but the adhesive property was not explored until 2007 as more and more attention was drawn to the area of synthetic mussel adhesive. This type of rediscovery seems to be a very common phenomenon. As discussed in Chapter 1, polyaniline was discovered 150 years ago, but until the past three decades, scientists didn't study deeply the chemical and physical properties of polyaniline as an excellent

conducting polymer. Another famous example is graphite oxide. This form of oxidized graphite was first reported in 1859 by Brodie [23] and modified by Hummer in 1958 [24]; however, it doesn't receive much attention until recently when people found out that it is an ideal precursor to prepare processable graphene. Actually people attempted to reduce graphite oxide as early as 1934.[25] If we had atomic force microscopy at that time, we would probably have seen chemically converted graphene prepared 80 years earlier!

(f) L-DOPA-like molecules can be attached to polyallylamine or polyacrylic acid through carbodiimide mediated amide coupling. The functionalized polymer can be used as pH-sensitive hydrogels or synthetic adhesives.[26-28]



Scheme 3.1 (i) Polyallylamine hydrochloride reacts with NaOH in methanol for 24 hours at r. t. to produce polyallylamine base solution. (ii) Polyallylamine base reacts with dihydroxybenzaldehyde in methanol for 2 hours to form Schiff's base. (iii) Schiff's base is reduced by NaBH<sub>4</sub> in methanol. (iv) The product is purified by dialysis against 1mM HCl.



The listed examples show the diversity of uses for synthetic mussel adhesives. They can be synthesized with a proper combination of polymer backbone, lots of L-DOPA residues, other desirable functional groups with some decent processability. The prepared polymers are not limited to adhesion, but also other useful applications. For example, catechol-containing polyallylamine was synthesized as a new water-soluble synthetic mussel adhesive by simple chemistry (Scheme 3.1). The as-prepared synthetic polymer can adhere two glass slides together. The polymer crosslinks in alkaline aqueous solution and retains its adhesion strength, whereas the original polyallylamine dissolves in water quickly under the same condition.

### **3.2 Experimental Section**

#### *Polyallylamine Base Solution*

A 0.6 gram KOH pellet was dissolved in 10 ml of methanol. 1 g of polyallylamine hydrochloride was added to the solution. The mixture was stirred for 24 hours at room temperature. The solution was then filtered and the precipitate washed with another 10 ml of methanol. The filtrate was collected for next step.

#### *Poly[N-(3,4-dihydroxybenzylidene)allylamine]*

1.47 grams 3,4-dihydroxybenzaldehyde was dissolved in 10 ml methanol and added dropwise into the polyallylamine base solution from the previous step. A yellow precipitate forms immediately. The reaction was carried out at room temperature for 2 hours. The yellow product was filtered and washed with more methanol. The product was then dried under vacuum oven at room temperature overnight.

*Poly[N-(3,4-dihydroxybenzyl)allylamine-co-allylamine] (Synthetic Mussel Adhesive)*

0.5 gram poly[N-(3,4-dihydroxybenzylidene)allylamine] was suspended in 25 ml of methanol. 0.55 grams of NaBH<sub>4</sub> was added slowly into the suspension. The yellow suspension gradually dissolved in the methanol and the color changed to light red. The reaction was carried out for 1 hour at room temperature and then refluxed for half an hour to complete the reaction and consume all of the NaBH<sub>4</sub>. The solvent was removed under vacuum to obtain a solid mixture of product and sodium salt. The solid was then dissolved into 25 ml distilled water to obtain a slightly red solution. The aqueous solution was dialyzed against 10 mM HCl thoroughly. Red hydrogel forms during the first cycles of dialysis and dissolves again. The purified dialysis solution was freeze-dried to obtain the final product.

*Adhesion Testing*

3 inch by 1 inch microscopic glass slides were cleaned in dilute HNO<sub>3</sub>, washed with distilled water and dried in air. 30% synthetic mussel adhesive was prepared in distilled water to obtain a viscous slightly pink solution. 45 µl of adhesive solution and 15 µl of NaIO<sub>4</sub> as the cross-linking reagent (3: 1, catechol: cross-linker) were combined between two glass slides. Samples were cured at 50 °C for 24 hours. Polyallylamine was also tested as a control experiment.

*Borate Cross-linked Hydrogel*

30 mg of NaBH<sub>4</sub> was dissolved in 1 ml of methanol. The solution was heated to convert all the borohydride to tetramethoxyborate. Then 30 mg of synthetic mussel adhesive

polymer was added to obtain a red solution. The solvent was dried and the solid was re-dissolved in 1 ml of distilled water. The solution was transferred into a dialysis bag and dialysed against water overnight. A yellow/red transparent gel formed.

#### *Fe<sup>3+</sup> Cross-linked Hydrogel*

100  $\mu$ l of 5% synthetic mussel adhesive was combined with 5  $\mu$ l of FeCl<sub>3</sub> (3: 1, catechol: cross-linker). The color changed to blue/violet immediately. The combined solution was drop-cast onto a glass substrate and treated with ammonia gas to form a hydrogel. The solution became viscous in seconds and the color changed to dark red.

#### *Swelling Tests*

10 mg of synthetic mussel adhesive was dissolved in 0.1 ml distilled water, drop-cast onto a glass slide and dried to obtain a thick film. The glass slide was immersed into distilled water for 20 seconds. The dried film absorbed water and swelled up to form a hydrogel.

### **2.3 Results and Discussion**

Catechol functionalized polyallylamine and polyacrylic acid have been synthesized previously using carbodiimide activated acid/amine coupling.[26, 28] However, the low efficiency of these reactions make the final coupling degree less than 10%. In our synthesis, the catechol group is attached onto the backbone through the formation of Schiff base, which is very rapid and goes to completion. This intermediate Schiff base imine is not very stable in aqueous solution, especially under acidic conditions, and thus

is further reduced to secondary amines by sodium borohydride. The  $^1\text{H-NMR}$  spectrum (Figure 3.3) shows that the final product has about 55% of catechol groups. The remaining 45% charged amines help to solubilize the polymer in aqueous solution.

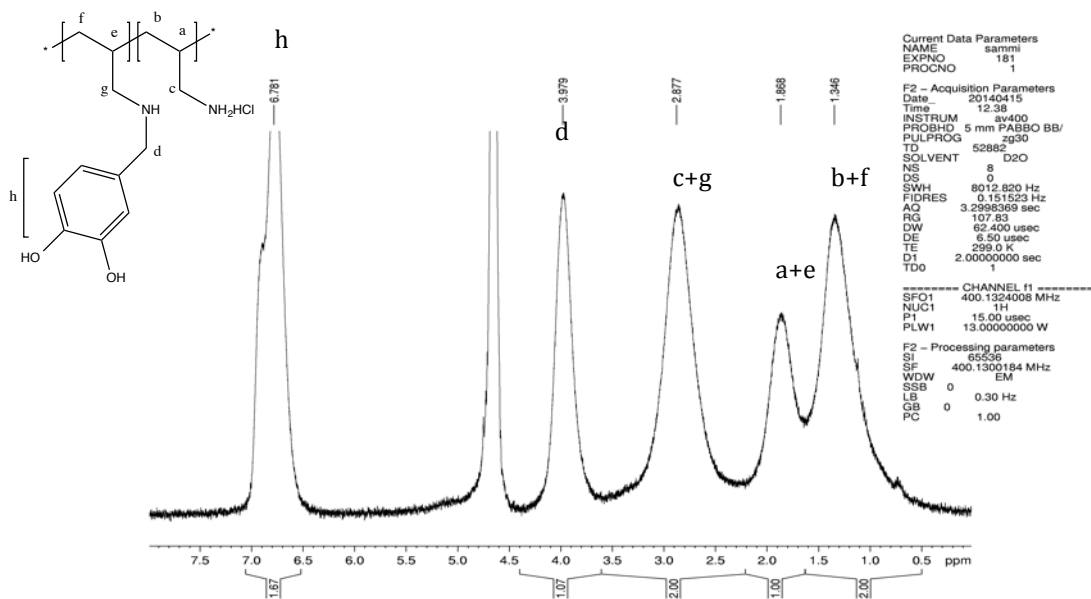


Figure 3.3  $^1\text{H-NMR}$  spectrum of synthetic mussel adhesive. The ratio between d and h is approximately 1.5. The slight difference is probably caused by some boron adduct formation during the reduction.

The molecular weight also plays an important role in the solubility. When larger polymers are used, the solubility decreases greatly. Consider that the most active mfp-3 and mfp-5 in mussel plaques both have low molecular weight; therefore, it is reasonable to use a low molecular weight polyallylamine as the starting material.

The intermediate Schiff's base is a yellow precipitate, which is hardly soluble in any common organic solvent. This is caused by certain interactions between the acidic hydroxyl groups and the amino groups (Figure 3.4).[29] When the suspension of this

yellow solid is treated with  $\text{NaBH}_4$ , it gradually dissolves into methanol to create a light red solution probably due to the formation of some charged borate complexes. After dialysis against  $\text{HCl}$ , the positively charged primary amines enable good solubility of the polymer in water. Catechol group tends to be oxidized by oxygen in the air especially under alkaline conditions. Thus, an inert gas or chemical protection has been used in many previous studies. During this synthesis, the nature of the reaction makes any protection unnecessary. First, the Schiff base is in the form of an insoluble solid caused by hydroxyl-amine interactions and thus inert to oxygen. Second, although the pH of the  $\text{NaBH}_4$  solution is above 7, the catechol group is protected by the generated borate complex. Third, the acidic dialysis conditions prevent the oxidation of the final polymer.

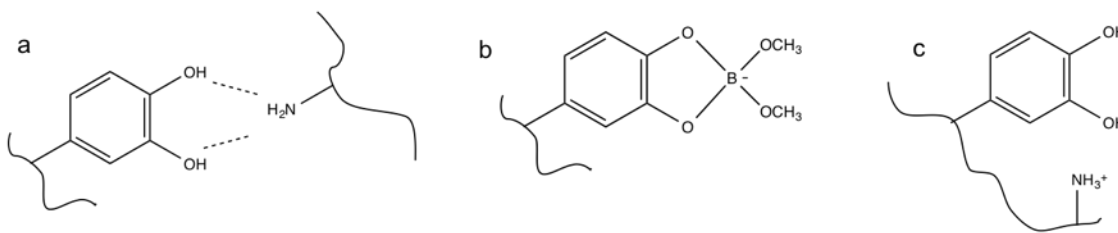


Figure 3.4 (a) Strong interaction between OH and  $\text{NH}_2$  precipitates the imine product. (b) The anionic borate complex solubilized polymer. (c) The positively charged final product is soluble in water.

Figure 3.5 shows the adhesion test of both the synthesized mussel adhesive mimic and the parent polymer polyallylamine with and without cross-linker. Both polymers can adhere two glass slides together and a vial full of water can be supported by the adhesion. When cross-linker is added to synthetic mussel adhesive, the color changes to dark red, which indicates the cross-linking of catechol groups. Too much cross-linking weakens the interfacial adhesion strength and the two glass slides can be pulled apart easily. However, when immersed in alkaline solution (diluted ammonium hydroxide), the glass slides

glued by polyallylamine separates within minutes due to the loss of charge; whereas, the slides adhered by the mussel mimic still hold together strongly. Moderate cross-linking under alkaline conditions are likely responsible for this water resistance.

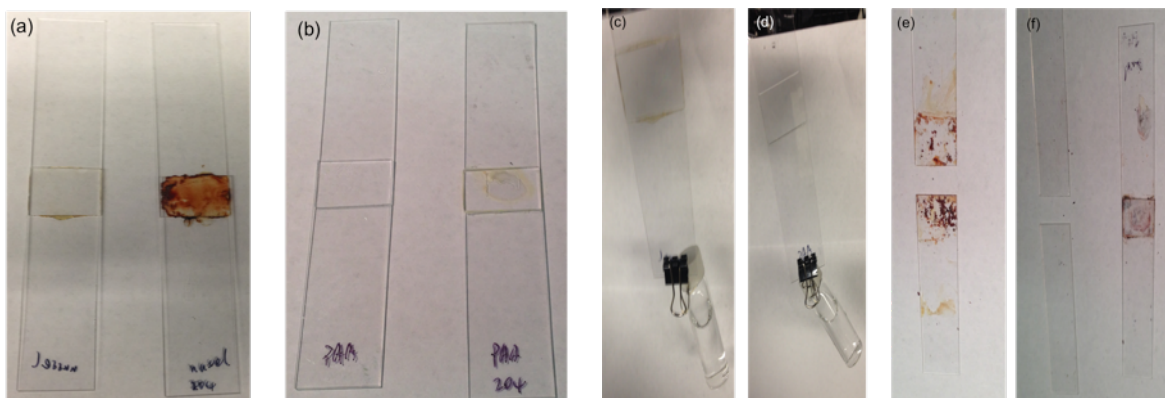


Figure 3.5 (a) Adhesion test of the mussel adhesive mimic with (right) and without (left) an oxidative cross-linker. (b) Adhesion test of polyallylamine with (right) and without (left) an oxidative cross-linker. (c) Synthetic mussel adhesive can hold a glass vial filled with water. (d) Polyallylamine can also hold a glass vial. (e) Oxidative cross-linking of catechol groups weakens the adhesion. (f) Polyallylamine (left) dissolves in alkaline water, while the synthetic mussel adhesive still holds the two glass slides together.

Catechol-containing polymers tend to form hydrogels with proper non-oxidative cross-linkers at a proper pH. When the synthetic mussel adhesive polymer is dialyzed during the purification process, it forms a hydrogel during the first cycles of dialysis (Figure 3.6a-c) and then dissolves in water again. This can be explained by the pH dependent complexation of borate with catechol [30]. Only mono-catechol complexes form at very high pH and the polymer is soluble in solvent in its anionic form. At moderately high pH (i.e. the first cycles of dialysis), bi-catechol complexes start to form and cross-link the polymer into a hydrogel. The removal of borate occurs at low pH, and the polymer dissolves into water again in the cationic form (Figure 3.6d). Compared to other similar

systems where 15% polymer is required, here 3% polymer is sufficient to form a homogeneous hydrogel probably because of the high percentage of catechol groups.

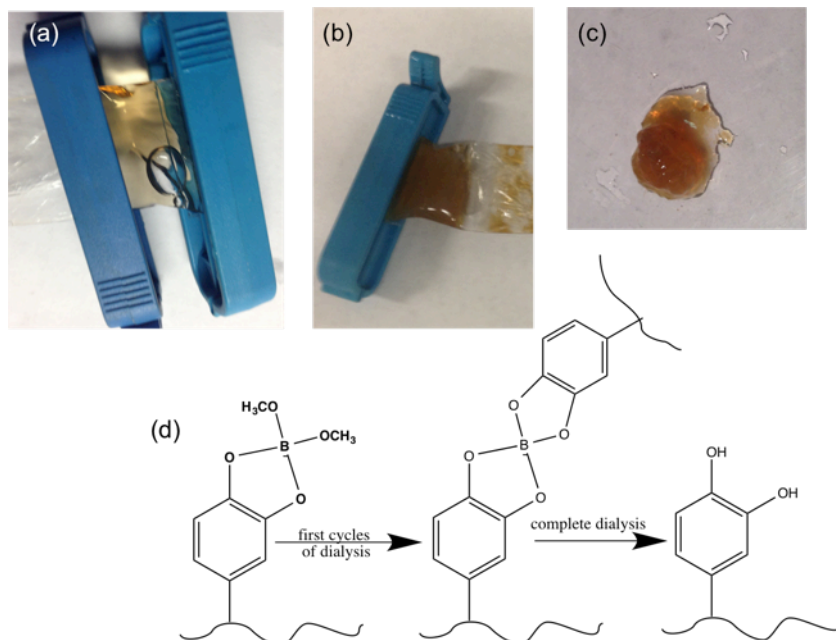


Figure 3.6 (a) Solution of mussel mimic and borate salt in water before dialysis; the nature of the borate salt makes the solution quite alkaline. (b, c) After overnight dialysis, the polymer solution becomes a homogeneous hydrogel. (d) The mechanism of hydrogel formation: from a mono-catechol complex at high pH (left) to a bi-catechol complex at moderate pH (middle) and finally to a borate-free catechol at low pH (right).

Another common cross-linker is ferric ion. When  $\text{FeCl}_3$  is added (catechol: cross-linker, 3 : 1) into the solution of adhesive mimic, the color changes to violet/blue because of the formation of a bi-dentate complex (Figure 3.7e). When the solution is exposed to ammonia vapor, the color changes to red within seconds, indicating the formation of a tri-catechol complex. The solution becomes viscous and hard forming a hydrogel (Figure 3.7a). Because of the high percentage of catechol group, 5% of the polymer is sufficient to form strong hydrogels. Similar to many other systems, this metal-coordinated hydrogel

exhibits the ability to self-heal: when two halves of cleaved hydrogels are pushed into contact again, they fuse together into one piece within minutes (Figure 3.7b-d).

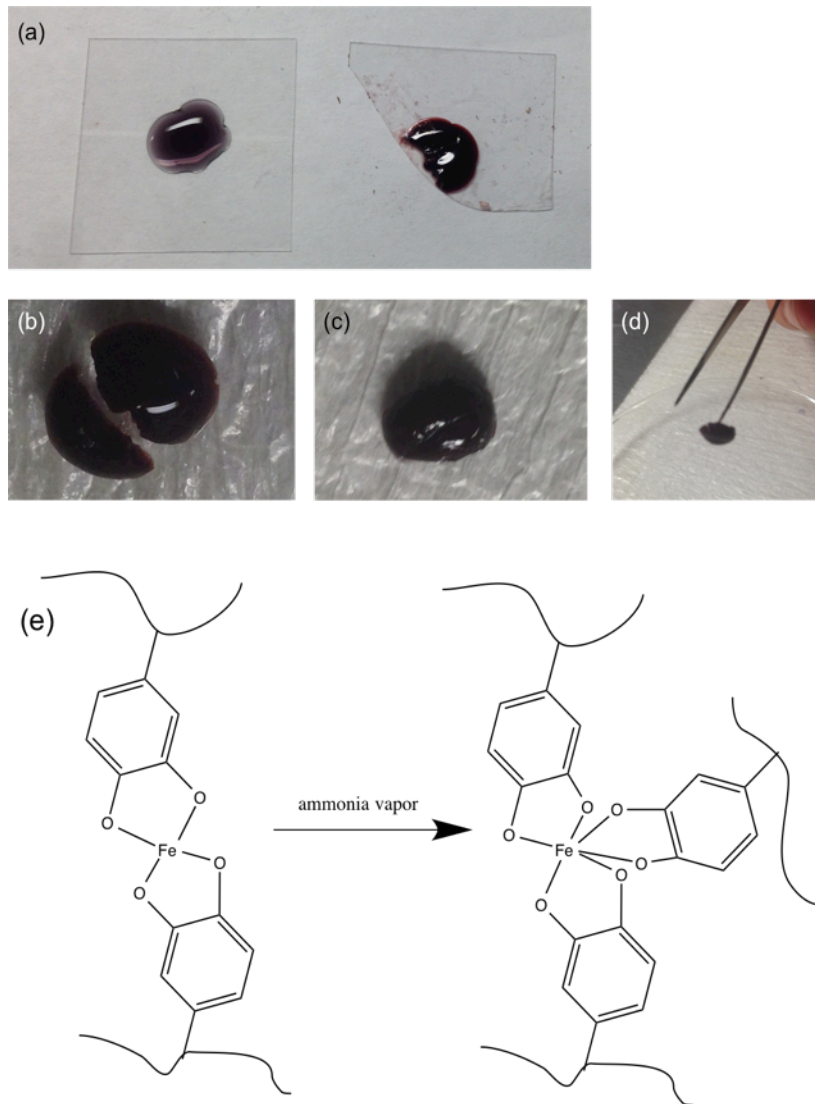


Figure 3.7 (a) When a 5% polymer solution is exposed to ammonia vapor, it becomes a red gel within seconds. (b) The formed hydrogel is then cut into two pieces. (c) When brought together the two halves fuse within minutes. (d) The self-healed hydrogel can then be lifted up. (e) The likely mechanism for hydrogel formation.



Another interesting property is swelling. When the dried film of synthesized polymer is immersed into neutral water, the film absorbs water and swells up to form a hydrogel (Figure 3.8). Covalently cross-linked polyallylamine or polylysine hydrogels also have swelling properties. But this one is not cross-linked, so the swelled hydrogel is supported by strong interchain and intrachain hydrogen bonding.



Figure 3.8 Left: dried polymer film. Right: when the film is dipped into water, it swells to form a gel.

### 3.4 Conclusions

A novel water-soluble synthetic mussel adhesive has been synthesized by attaching catechol groups onto polyallylamine. The functionalization degree is 55% and the remaining 45%, a charged primary amine, enables the polymer to become soluble in water. This synthetic mussel adhesive can adhere two glass slides together strongly and the adhesion is stable under alkaline conditions due to moderate self-crosslinking. Hydrogels can also be formed at very low concentrations by cross-linkers such as borate and ferric ions.

### s3.5 References

1. Nicholson et al. *History of Adhesives ESC Report* **1991**.
2. Pell Research - Adhesive Manufacturing.
3. Vasav Sahni, Todd A. Blackledge, and Ali Dhinojwala, *The Journal of Adhesion* **2001**, 87, 595.
4. Qi Lin, Delphine Gourdon, Chengjun Sun, Niels Holten-Andersen, Travers H. Anderson, J. Herbert Waite, and Jacob N. Israelachvili, *Proc. Natl. Acad. Sci.* **2007**, 104, 3782.
5. Review of Mussel Adhesion Mechanism and Scoping Study, Bureau of Reclamation, Technical Memorandum No. MERL-2013-43.
6. Qingye Lu, Eric Danner, J. Herbert Waite, Jacob N. Israelachvili, Hongbo Zeng and Dong Soo Hwang, *J. R. Soc. Interface* **2013**, 10, 20120759.
7. Peter A. Suci and Gill G. Geesey, *Journal of Colloid and Interface Science*, **2000**, 230, 340.
8. James D. White and Jonathan J. Wilker, *Macromolecules* **2011**, 44, 5085.
9. Heather G. Silverman, Francisco F. Roberto, *Marin Biotechnology*, **2007**, 9, 661.
10. Bruce P. Lee, Jeffrey L. Dalsin, Philip B. Messersmith, *Biological Adhesives*, **2006**, 257.
11. Yu, M.; Deming, T. J. *Macromolecules* **1998**, 31, 4739.
12. Glass, P.; Chung, H. Y.; Washburn, N.R. *Langmuir* **2009**, 25, 6607.
13. Chung, H. Y.; Glass, P.; Pothen, J. M.; Sitti, M.; Washburn, N. R. *Biomacromolecules* **2011**, 12, 342.
14. Wang, J. J.; Tahir, M. N.; Kappl, M.; Tremel, W.; Metz, N.; Barz, M.; Theato, P.; Butt, H. J. *Adv. Mater.* **2008**, 20, 3872.
15. Zahid Shafiq, Jiayi Cui, Lourdes Pastor-Perez, Verónica San Miguel, Radu A. Gropeanu, Cristina Serrano, and Arjunzazu del Campo, *Angew. Chem. Int. Ed.* **2012**, 51, 4332.
16. Finlay, A. S.; Dalsin, J.; Callow, M.; Callow, J. A.; Messersmith, P. B. *Biofouling* **2006**, 22, 391.

17. Dalsin, J. L.; Lin, L. J.; Tosatti, S.; Voros, J.; Textor, M.; Messersmith, P. B. *Langmuir* **2005**, 21, 640.
18. Lee, H.; Lee, K. D.; Pyo, K. B.; Park, S. Y.; Lee, H. *Langmuir* **2010**, 26, 3790.
19. Yanlan Liu, Kelong Ai, and Lehui Lu, Polydopamine and Its Derivative Materials: Synthesis and Promising Applications in Energy, Environmental, and Biomedical Fields, *Chem. Rev.* ASAP Article.
20. Westwood, G.; Horton, T. N.; Wilker, J. J. *Macromolecules* **2007**, 40, 3960.
21. Cristina R. Matos-Pérez, James D. White, and Jonathan J. Wilker, *J. Am. Chem. Soc.* **2012**, 134, 9498.
22. Daly, W. H.; Moulay, S. *J. Polym. Sci.* **1986**, 74, 227.
23. B. Brodie, *Phil. Trans.* **1859**, 149, 249.
24. Hummers, W. S.; Offeman, R. E. *J. Am. Chem. Soc.* **1958**, 80, 1339.
25. Die Reduktion von Graphitoxyd mit Schwefelwasserstoff, *Colloid and polymer science*, **1934**, 68, 149.
26. Marie Krogsgaard, Manja A. Behrens, Jan Skov Pedersen, and Henrik Birkedal, *Biomacromolecules* **2013**, 14, 297.
27. Zahra Mohammadi, Sheng-Xue Xie, Allison L. Golub, Stevin H. Gehrke, Cory Berkland, *J. Appl. Polym. Sci.* **2010**, 121, 1384.
28. Li Jie Duan, Ying Liu, Jiheung Kim, Dong June Chung, *J. Appl. Polym. Sci.* **2013**, 131.
29. Eizo Oikawa and Ken Yahata, *Polymer Bulletin*, **1987**, 17, 315.
30. Maurice Padeloup and Colette Brisson, *Org. Magn. Resonance*, **1981**, 16, 164.

## **Chapter 4 Polyaniline-Based Electrically Conductive Synthetic Mussel Adhesive**

### **4.1 Introduction**

In Chapter 3, we discussed catechol containing synthetic mussel adhesives prepared by various chemistry methods. All these synthetic polymers based on polyacrylamide, polyethyleneglycol and polyallylamine show some kind of underwater adhesion due to the catechol groups. Thus, it will be interesting to incorporate groups into polyaniline to make conducting synthetic mussel adhesive.

Electrically conductive adhesives are actually already commercial available and widely used for electronics to bond and seal electronic components, to connect a circuit or to avoid charging of SEM samples (like SEM carbon tapes and copper tapes). All these conductive adhesives are made of two components — a conductive component and an adhesive component. The conductive component can be silver, copper, graphite or other unusual conductors; the adhesive component is generally a polymer resin that glues the whole system together. The conductive fillers are suspended in the adhesive component and contact each other to form conductive pathways in the adhesive.

Recent studies on novel conductive adhesives are also based on two-component systems. For example, the conducting polyurethane synthesized in Chapter 2 can also be viewed as a conductive adhesive. Conducting polyaniline/carbon nanotubes disperse homogeneously in polyurethane, which shows strong adhesion to substrates. Mixed graphite oxide and PEDOT: PSS turn into a sticky hydrogel that can glue glass slides

together. [1] PEDOT: PSS functions as conductive filler and graphite oxide rich in hydroxyl groups acts as a sticky component. Other sticky molecules can also be mixed with a PEDOT: PSS aqueous solution to make transparent electronic glue.[2] Although it is simple to mix polyaniline and a synthetic adhesive in this way to prepare a two-component electrically conductive adhesive, it would be very exciting to attach catechol groups to a polyaniline backbone by chemical modifications to obtain a one component conductive synthetic mussel adhesive.

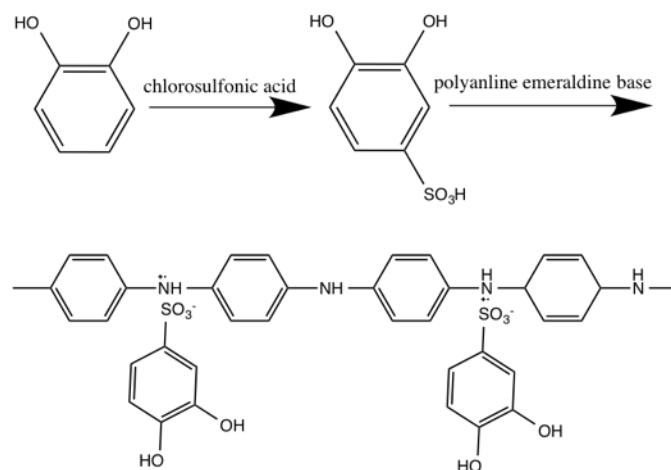
As mentioned earlier, polyaniline has a rich polymer chemistry. Polyaniline can be chemically tailored by various methods to achieve the desired chemical and physical properties. Aniline derivatives with various functional groups are commercially available at low cost. The polymerization and copolymerization of these monomers can be carried out by simple oxidative chemical polymerization. Functional groups or side chains can also be attached onto the polyaniline backbone through post modification. Dopants also play an important role on the properties of polyaniline. Although modified polyaniline usually loses some of its conductivity, not all applications require a high conductivity in the range of 10-1000 S/cm, Conductivity between  $10^{-1}$  and  $10^{-4}$  S/cm is still reasonable for a wide variety of potential applications.

In this chapter, different methods are tried to chemically modify polyaniline. Compared to the two-component system, there are some new difficulties that need to be solved. First of all, the requirement of conductivity excludes many polyaniline derivatives. Second, the

final polymer should be processable in at least in one solvent. Third, the product should show some kind of adhesion, which is not only determined by the catechol group.

#### **4.2 Polyaniline Doped with 3,4-dihydroxybenzenesulfonic Acid**

As mentioned above, any modification of the polyaniline backbone generally will be detrimental to the conductivity. Thus, a strong acid dopant with catechol moieties seems a smart way to avoid losses in conductivity. Common organic dopants are carboxylic acids or sulfonic acids. Although catechol containing carboxylic acids are commercially available at low cost, the high  $pK_a$  makes them poor dopants for polyaniline. The simplest sulfonic acid with a catechol moiety is 3,4-dihydroxybenzenesulfonic acid (Scheme 4.1). The chemical is synthesized based on the method of S. Saito et al.[3] In a typical synthesis, 1.1 grams of catechol is dissolved in 5 ml of anhydrous dimethyl carbonate. The solution is stirred in an ice bath. Then a solution of 1 equivalent of chlorosulfonic acid in 3 ml of dimethyl carbonate is added drop-wise to the catechol solution and the mixture is stirred in an ice bath for 2 hours and then at room temperature for another 12 hours. The solvent is evaporated under vacuum to full dryness to obtain a slightly pink solid after purification. The product is deliquescent and thus must be kept in a desiccator.



Scheme 4.1 Synthesis of 3,4-dihydroxybenzenesulfonic acid and the doping of polyaniline emeraldine base.

Figure 4.1 shows the proton NMR spectrum of as-synthesized 3,4-dihydroxybenzenesulfonic acid in methanol-d<sub>4</sub>. There is a little bit of solvent residue peak and impurity peaks probably from other isomers (the purity is around 90-95% based on the NMR), but this should be pure enough to use as a catechol containing dopant. The dopant can be oxidized easily even under acidic conditions, so it cannot be used during the oxidative polymerization. A polyaniline film doped with 3,4-dihydroxybenzenesulfonic acid has a conductivity comparable to the one doped with HCl.

Two methods were tried to test the adhesiveness of this dopant. In the first method, polyaniline emeraldine base and the synthesized dopant (monomer: dopant = 2: 1) were mixed and sonicated in a proper solvent such as DMSO, formic acid to obtain a concentrated dispersion. A controlled amount of the solution is applied between two substrates (glass, mica or aluminum) and cured at 50 °C for 24 hours. Unfortunately, after

the evaporation of the solvent, the dried doped polyaniline cannot glue the substrates together. They separate easily without any external force.

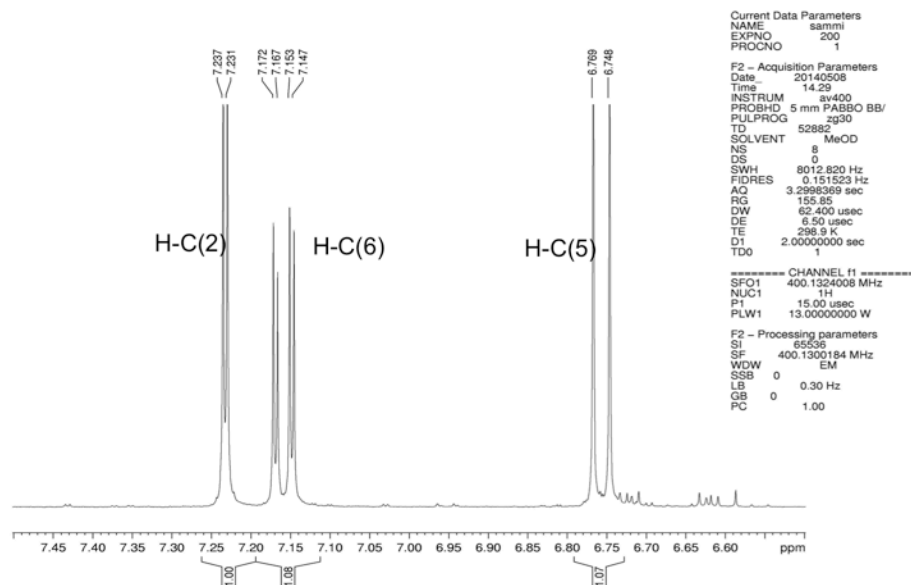


Figure 4.1  $^1\text{H}$  NMR spectrum of 3,4-dihydroxybenzenesulfonic acid ( $\text{CD}_3\text{OD}$ ).

In the second test, polyaniline emeraldine base is first dissolved in NMP to obtain a 2% solution. 1 ml of the prepared solution is dropcast onto a 1 inch by 1 inch glass slide and dried at 50 °C in a vacuum oven to obtain a thick film, which can be peeled off easily. The polyaniline film is then immersed in a 10% solution of 3,4-dihydroxybenzenesulfonic acid for 24 hours to be fully doped. The doped polyaniline film has a comparable conductivity to the film doped with HCl. However, the doped film is not sticky like other adhesive tapes and shows no adhesion to substrates like glass, mica or aluminum.



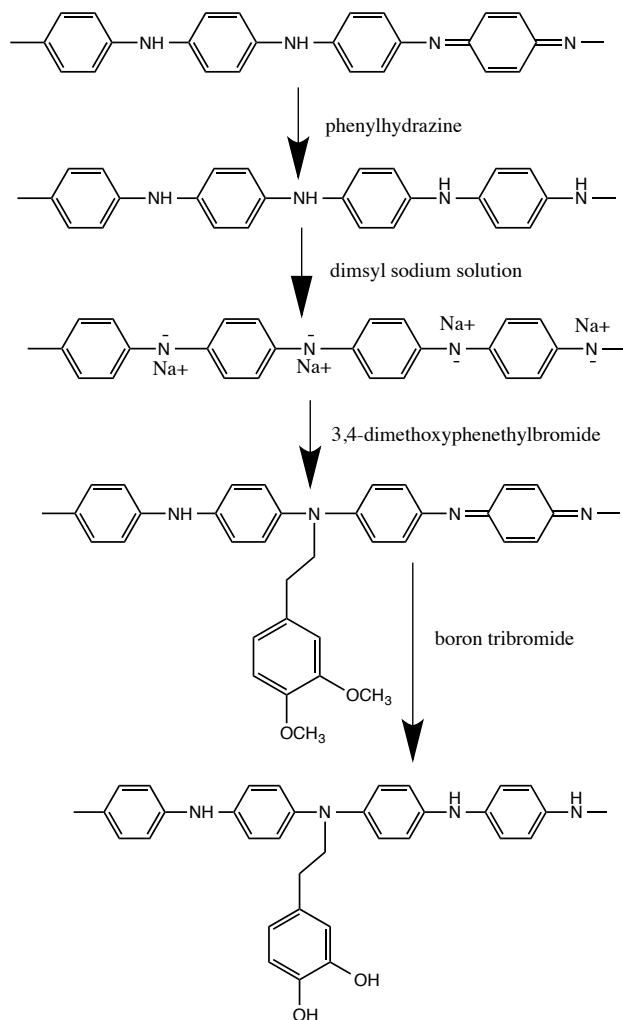
In summary, 3,4-dihydroxybenzenesulfonic acid was synthesized successfully and used as a dopant for polyaniline. Although the doped polyaniline shows a high conductivity, it cannot adhere to substrates like glass, mica and aluminum or glue two substrates together.

### **4.3 N-alkylation of Polyaniline with Catechol Containing Functional Groups**

Although polyaniline derivatives can be obtained from the corresponding substituted monomers, the prepared polymers suffer inherent physical limitations. Alkyl-ring substituted [4, 5] and alkoxy-ring [6]-substituted polyanilines after acid doping have a moderate conductivity of  $10^{-1}$ - $10^{-3}$  S/cm. They also have low molecular weights, on the order of  $10^3$ , and therefore, their mechanical strengths are relatively poor. Poly(N-alkylaniline)s have moderate molecular weights (about  $10^4$ ), however, their conductivities are low ( $10^{-4}$ - $10^{-7}$  S/cm). [7, 8] One way to solve both problems is to post-functionalize polyaniline with a desired molecular weight. N-alkylated polyanilines have been synthesized by incorporation of flexible alkyl chains onto the polyaniline through N-alkylation methods [9-11]. The functionalized polyaniline usually has better solubility in common organic solvents. Both leucoemeraldine and emeraldine polyaniline can be used as starting materials. While the former can maximize the degree of substitution, the latter always results in much higher conductivity ( $10^{-1}$ - $10^{-3}$  S/cm) due to higher oxidation levels since the imine nitrogens are available for acid doping.

In this section, an alkylation reagent with catechol residues is used to functionalize polyaniline. (Scheme 4.2) Because of the nucleophilicity of the hydroxyl groups, the

catechol moiety is protected during the N-alkylation process. The deprotection can be achieved by refluxing in HBr or boron tribromide at room temperature. [12, 13] Compared to much more flexible aliphatic alkyl chains, the steric hindrance will decrease the degree of substitution. Thus, the leucoemeraldine base is used in the alkylation step to maximize the degree of substitution.



Scheme 4.2 N-alkylation of polyaniline. To maximize the degree of substitution, polyaniline is first reduced to the leucoemeraldine state. The amine group is deprotonated by dimethyl ion and functionalized by an alkyl halide. The deprotection of the catechol group is carried out in a boron tribromide solution.

### *Synthesis of Leucoemeraldine Base Polyaniline*

Polyaniline in its emeraldine oxidation state was synthesized and purified by a rapid mixing method [14]. The fully reduced form of polyaniline was obtained by reduction with excess phenylhydrazine in methanol for 48 hours. The collected gray-white powder was washed with THF to remove any excess reducing agent. To avoid oxidation, the leucoemeraldine polyaniline was stored under an inert gas.

### *Preparation of Dimsyl Sodium Solution*

160 mg of NaH (a 60% dispersion in mineral oil) was added to a 100 ml Schlenk flask. The mineral oil was washed away using pentane three times. The color of the NaH solid changed from gray to white. The solvent residue was boiled off under vacuum and the flask was purged with argon three times. 25 ml of anhydrous DMSO was added to the flask and the mixture was stirred at 50 °C until the NaH was fully dissolved to obtain a milky yellow dimsyl sodium solution.

### *Preparation of N-alkylated Polyaniline*

500 mg of polyaniline in its leucoemeraldine form was added to the dimsyl sodium solution prepared above. The deprotonation of the secondary amine group was carried out at 40 °C for 1 hour under argon. The polymer gradually dissolved in the solvent and the color of the solution changed to dark brown. An excess amount of 3,4-dimethoxyphenethylbromide dissolved in DMSO was slowly added to the solution. The color of the solution gradually changed to dark blue and the alkylated polyaniline precipitated. The reaction was carried out at 40 °C overnight and the precipitate was

filtered, washed thoroughly with methanol and acetone and then dried at 40 °C in a vacuum oven.

Figure 4.2 shows the proton NMR spectrum of N-alkylated polyaniline in DMSO-d<sub>6</sub>. The as-synthesized functionalized polyaniline was intractable and hardly soluble in any common solvents. There is very small percentage of polymer that dissolved in DMSO and the soluble portion shows that the degree of substitution is only 7%. My best guess is that the insoluble part has a higher degree of substitution and the strong inter-/intra-chain interactions such as hydrogen bonding makes the product intractable. Due to the solubility problem, the de-protection step was not carried out.

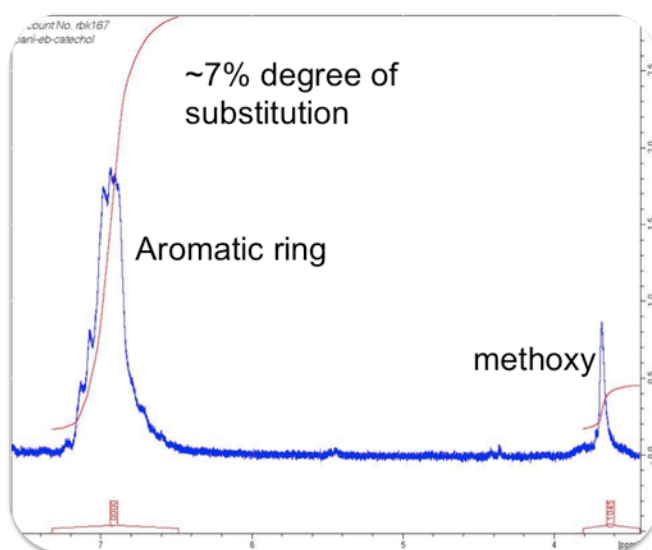
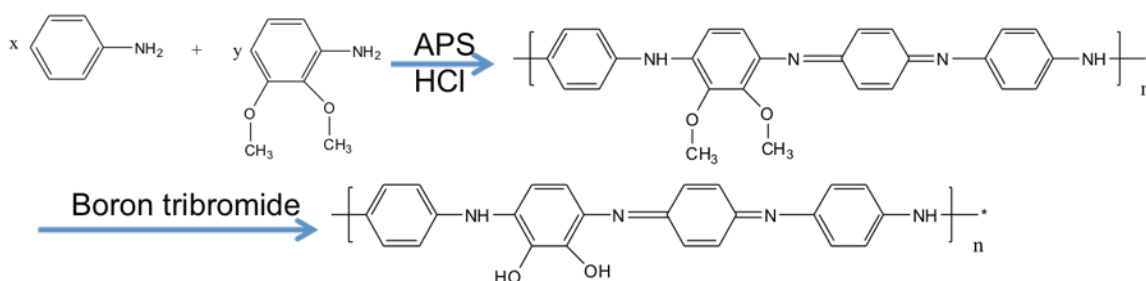


Figure 4.2 <sup>1</sup>H NMR spectrum of N-alkylated polyaniline in DMSO-d<sub>6</sub>. The solubility of the polymer is very low and the soluble part shows that the degree of substitution is only 7%.

#### 4.4 Poly(2,3-dihydroxyaniline-co-aniline)

Poly(2,3-dihydroxyaniline-co-aniline) (Scheme 4.3) has a similar structure to poly(3,4-dihydroxystyrene-co-styrene) [15], which has proved to be a good adhesive as strong as commercially available superglue. Scheme 4.3 demonstrates the method of synthesis. The

polymer can be synthesized by a simple chemical oxidative polymerization just as other polyaniline derivatives. However, the 2,3-dimethoxyaniline was used during polymerization because of the reactivity of the hydroxyl groups. The demethylation is supposed to be done with boron tribromide.



Scheme 4.3 Synthesis of poly(2,3-dihydroxyaniline-co-aniline).

Like other alkyl-ring substituted polyanilines, the conductivity and molecular weight decreased due to the steric hindrance of the functional group. Actually the homopolymerization of 2,3-dimethoxyaniline only results in red oligomers with low yield. Copolymerization with polyaniline can partially overcome this problem. Table 4.1 shows the sheet resistance of the copolymer with different ratios. The resistance of the copolymer begins to climb into a reasonable range when the percentage of aniline is above 80%. Table 4.1 also shows that the copolymer composition is close to the feed composition. Thus the reactivity of two monomers during polymerization is similar. The failure of homopolymerization of 2,3-dimethoxyaniline is likely because of the crowded side groups (both ortho and meta positions are occupied). The methoxy groups increase the solubility of the copolymer in less polar organic solvents such as dichloromethane. The de-protection was carried out by boron tribromide in dichloromethane. However, the resulting pink precipitate was insoluble in all common solvents. Thus, the structure and

the adhesion ability could not be investigated.

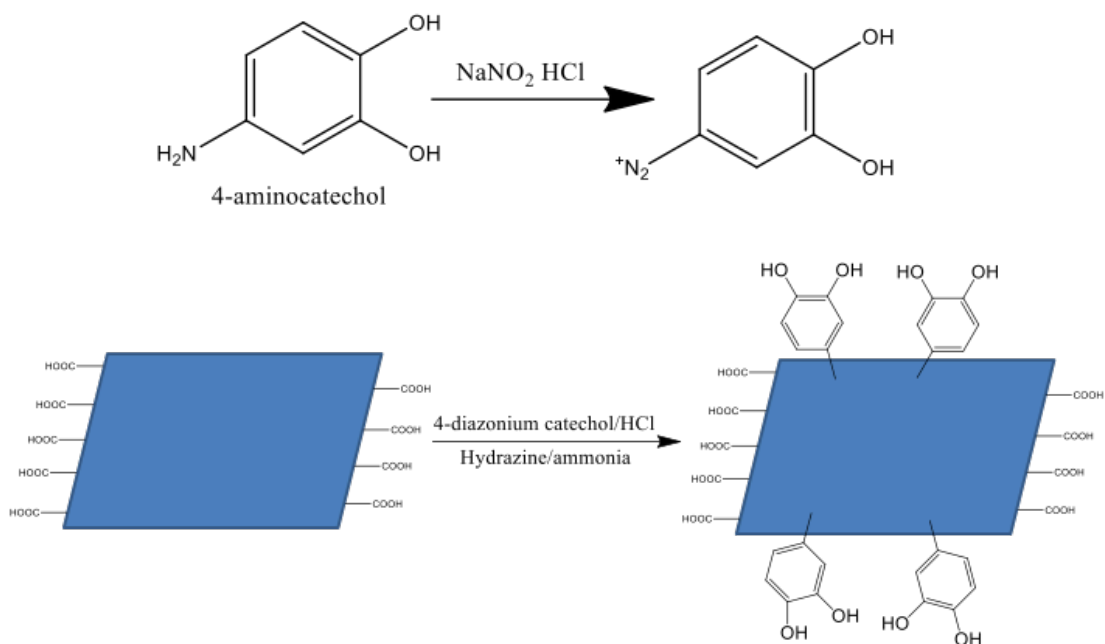
Table 4.1 Composition and sheet resistance of poly(2,3-methoxyaniline-co-aniline). DMOA is short for 2,3-dimethoxyaniline. The ratio of the two monomers was calculated from the proton NMR spectrum.

Aniline:DMOA	Pure aniline	9:1	4:1	1:1	Pure DMOA
% of methoxy protons	0	12	76	57	68
% of aromatic protons	100	88	24	39	32
% of DMOA	0	10	20	68	94
Sheet Resistance	7 Kohm	500 Kohm	4 Mohm	-	-

#### 4.5 Catechol Functionalized Graphene

Graphene, a single-atom-thick sheet of hexagonally arrayed  $sp^2$ -bonded carbon atoms, is a recently discovered conducting material. It shares many similar chemical properties to carbon nanotubes, which can be viewed as one or few layers of scrolled graphene sheets. Previous work has shown that aryl diazonium treatment of graphene produces functionalized graphene. [16-18] Although this functionalization will lower the conductivity due to the loss of  $sp^2$  conjugation, the functionality expands the applications of graphene. In this section, aqueous dispersions of catechol functionalized chemically

converted graphene is synthesized (Scheme 4.4) and the adhesive force is tested by atomic force microscopy (AFM).



Scheme 4.4 Catechol-4-diazonium salt can be prepared in HCl with NaNO<sub>2</sub>. It can react with the sp<sup>2</sup> regions of chemically converted graphene to attach catechol groups onto the graphene surface.

#### *Synthesis of 4-aminocatechol HCl Salt*

Aminocatechol was prepared according to a previous report [20]. 4-Nitrocatechol (2 g) was suspended in 10 ml of water and mixed with 5 g of granulated tin. Concentrated HCl was added in 3 portions of 10 ml each and the mixture then heated on a boiling water bath. The excess tin was removed by filtration and the filtrate was diluted with distilled water and treated with hydrogen sulfide. The solution was filtered to remove tin sulfide and the filtrate was evaporated until crystals of the HCl salt began to form. The solution was then left in the cold room overnight; the crystals were filtered off, dissolved in a minimum volume of water and recrystallized. The structure was confirmed by proton NMR (Figure 4.3).

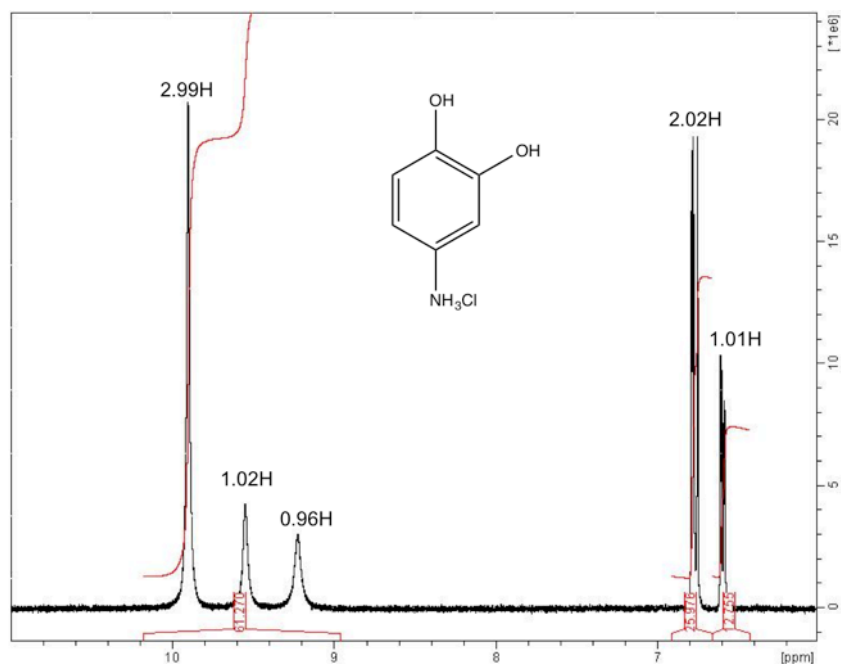


Figure 4.3 <sup>1</sup>H NMR spectrum of 4-aminocatechol HCl salt.

### *Synthesis of Chemically Converted Graphene (CCG) Dispersions*

The synthesis follows Dan Li's method [19]. In a typical synthesis, graphite oxide prepared by a modified Hummer's method was dissolved in 50 ml of distilled water to create a 0.2 mg/ml dispersion. Next, 175  $\mu$ l of 28% ammonium hydroxide was added to the dispersion to adjust the pH to around 10. Then, 70  $\mu$ l 10% of a hydrazine solution was added to the mixture. This reaction was carried out at 90 °C for 1 hour. The color of the solution changed gradually from light brown to dark black.

### *Catechol Functionalized Graphene Dispersions*

15 mg of a 4-aminocatechol HCl salt was dissolved in 1 ml of 0.3 molar HCl and 6 mg of NaNO<sub>2</sub> was dissolved in 1 ml of distilled water. The two solutions were chilled in an ice bath and then the NaNO<sub>2</sub> solution was added drop-wise into the 4-aminocatechol solution. The color changed to red immediately. The mixture was stirred in an ice bath



for 10 minutes. Then the solution was added to 20 ml of a CCG dispersion prepared above. The reaction was carried out at room temperature for 1 hour and dialyzed against 1 mM HCl. In a control experiment, the solution of 4-aminocatechol was added directly into the CCG dispersion and dialyzed against HCl;

The successful functionalization was confirmed in three ways. (Figure 4.4) First, the functionalized CCG shows good dispersibility in water, while the control precipitates. Second, cyclic voltammetry curves showed the redox peaks of the catechol group for the functionalized CCG, while the control experiment did not. Third, both samples were drop-cast onto glass slides to obtain thin films. The control had a sheet resistance comparable to CCG, whereas the functionalized one had a higher resistance due to the damaged  $sp^2$  conjugation.

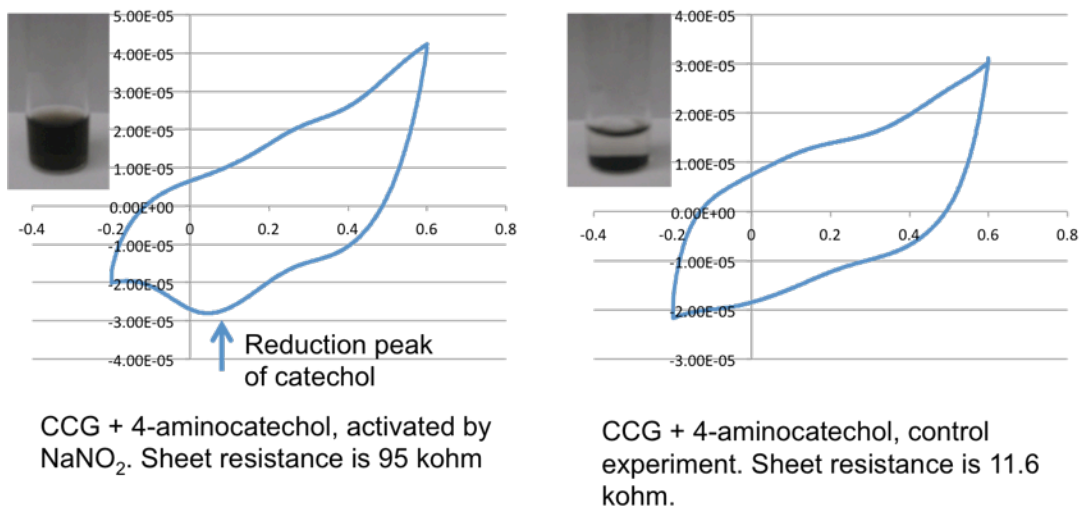


Figure 4.4 Left: catechol functionalized graphene exhibits its characteristic reduction peak in a CV curve. The functionality increases the dispersibility of graphene in water, but decreases the conductivity. Right: a control experiment shows no redox peaks. The conductivity is the same as CCG, because of no chemical modification. Graphene precipitates due to the salt effect.

### Adhesiveness Test by AFM

The surface adhesion force of the functionalized CCG can be measured by AFM. Figure 4.5 illustrates the mechanism of the adhesion measurement. Unfortunately, there is no big difference among the CCG, functionalized CCG and the control experiment.

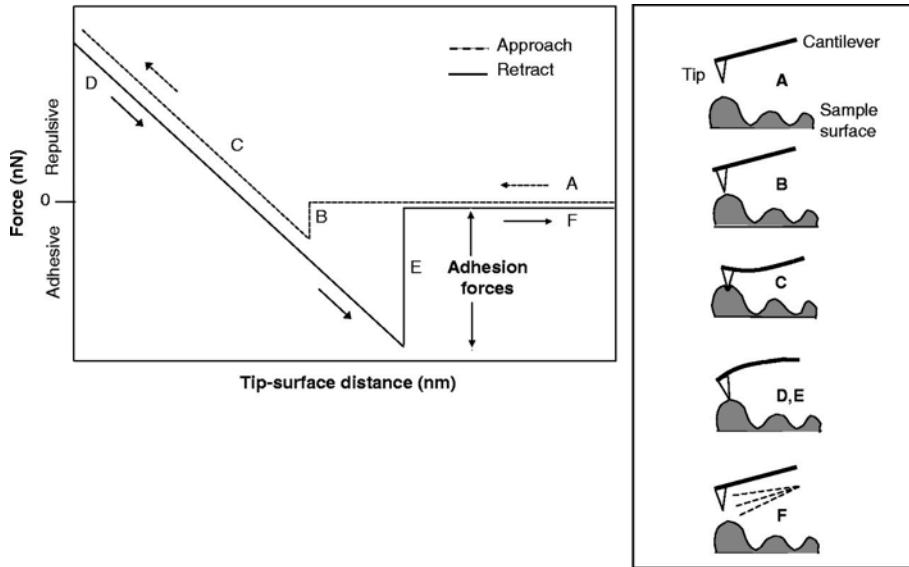


Figure 4.5 Force-distance curves describing a single approach-retract cycle of the AFM tip. The AFM tip approaches the sample surface (A). The initial contact between the tip and the surface is mediated by the attractive van der Waals forces (contact) that lead to an attraction of the tip toward the surface (B). Hence, the tip applies a constant and default force upon the surface that leads to sample indentation and cantilever deflection (C). Subsequently, the tip tries to retract and to break loose from the surface (D). Various adhesive forces between the sample and the AFM tip, however, hamper tip retraction. These adhesive forces can be taken directly from the force-distance curve (E). The tip withdraws and loses contact to the surface upon overcoming of the adhesive forces (F). The original picture was published in *J Cell Sci.* **118**, 2881-2889.

### 4.6 Conclusions

Different methods have been tried to graft catechol groups onto conducting materials such as polyaniline and graphene in order to prepare novel conductive adhesives. The

difficulty is to balance simultaneously the properties of conductivity, solubility and adhesiveness. Some methods do modify the conducting material successfully, but they do not show any obvious adhesion.

## 4.7 References

1. Vincent C. Tung, Jaemyung Kim, Laura J. Cote, and Jiaxing Huang, *J. Am. Chem. Soc.* **2011**, 133, 9262.
2. Jianyong Ouyang and Yang Yang, *Adv. Mater.* **2006**, 18, 2141.
3. Shizuka Saito and Jun Kawabata, *Helvetica Chimica Acta* **2006**, 89, 1395.
4. M. Leclerc, J. Guay and L.H. Dao, *Macromolecules* **1989**, 22, 649.
5. Y. Wei, W.W. Focke, G.E. Wnek, A. Ray and A.G. MacDiarmid, *J. Phys. Chem.* **1989**, 93, 495.
6. D. Macinnes and B.L. Funt, *Synth. Met.* **1988**, 25, 235.
7. Chevalier, J. W.; Bergeron, J. Y.; Dao, L. H. *Macromolecules*, **1992**, 25, 3325.
8. Wei, Y.; Focke, W. W.; Wnek, G. E.; Ray, A.; MacDiarmid, A. G. *J. Phys. Chem.* **1989**, 93, 495.
9. Wen-Yue Zheng and Kalle Levon, *Macromolecules* **1994**, 27, 7754.
10. Gue-Wuu Hwang, Kuan-Ying Wu, Mu-Yi Hua, Hsun-Tsing Lee, Show-An Chen, *Synthetic Metals* **1998**, 92, 3946.
11. Mikhael, M. G., Padias, A. B. and Hall, H. K., *J. Polym. Sci. A Polym. Chem.*, **1997**, 35, 1673.
12. Yang, Z.; Pelton, R. *Macromol. Rapid Commun.* **1998**, 19, 241.
13. Daly, W. H.; Moulay, S. *J. Polym. Sci.* **1986**, 74, 227.
14. Jiaxing Huang and Richard B. Kaner, *Angew. Chem.* **2004**, 116, 5941.
15. Westwood, G.; Horton, T. N.; Wilker, J. J. *Macromolecules* **2007**, 40, 3960.
16. Jay R. Lomeda, Condell D. Doyle, Dmitry V. Kosynkin, Wen-Fang Hwang, and James M. Tour, *J. Am. Chem. Soc.* **2008**, 130, 16201.
17. Wei Gao, Mainak Majumder, Lawrence B. Alemany, Tharangattu N. Narayanan, Miguel A. Ibarra, Bhabendra K. Pradhan and Pulickel M. Ajayan, *ACS Appl. Mater. Interfaces* **2011**, 3, 1821.
18. Yongchao Si and Edward T. Samulski, *Nano Lett.* **2008**, 8, 6.

19. Li, D., Muller, M. B., Gilje, S., Kaner, R. B. & Wallace, G. G., *Nature Nanotechnology*, **2008**, 3, 101.

20. P. J. Wright and D. T. Plummer, *Biochemical Pharmacology*, **1974**, 23, 65.

## **Chapter 5 Solvothermal Reduced Graphene Oxide Dispersions in Organic Solvents**

Graphene is a single-atom-thick sheet of  $sp^2$ -bonded carbon atoms and can be viewed as a single layer of graphite. Although the theoretical study of graphene, a single hexagonal layer was explored by P. R. Wallace as early as 1947 [1], the experimental isolation was not successful until 2004 when Novoselov, Geim and coworkers at the University of Manchester peeled off graphene layers from graphite and transferred them onto a  $SiO_2/Si$  wafer. [2] They shared the 2010 Nobel Prize in Physics for this discovery. Early studies revealed many interesting properties of graphene such as an ambipolar field effect [2], the quantum Hall effect at room temperature [3, 4] and measurements of extremely high carrier mobility [5, 6]. These properties drew huge interest from scientists and engineers in the synthesis and implementation of graphene. Although the ‘peel-off’ method produces the highest quality graphene, it cannot be scaled up for widespread applications. Large-scale graphene, however, can be prepared through chemical methods using graphite oxide (Figure 5.1) as an intermediate. Although the quality of chemically converted graphene is inferior to graphene produced by the peel-off method or by a chemical vapor deposition method, it can be treated as a large carbon-based macromolecule, which shares many similar chemical properties to carbon nanotubes and fullerenes.

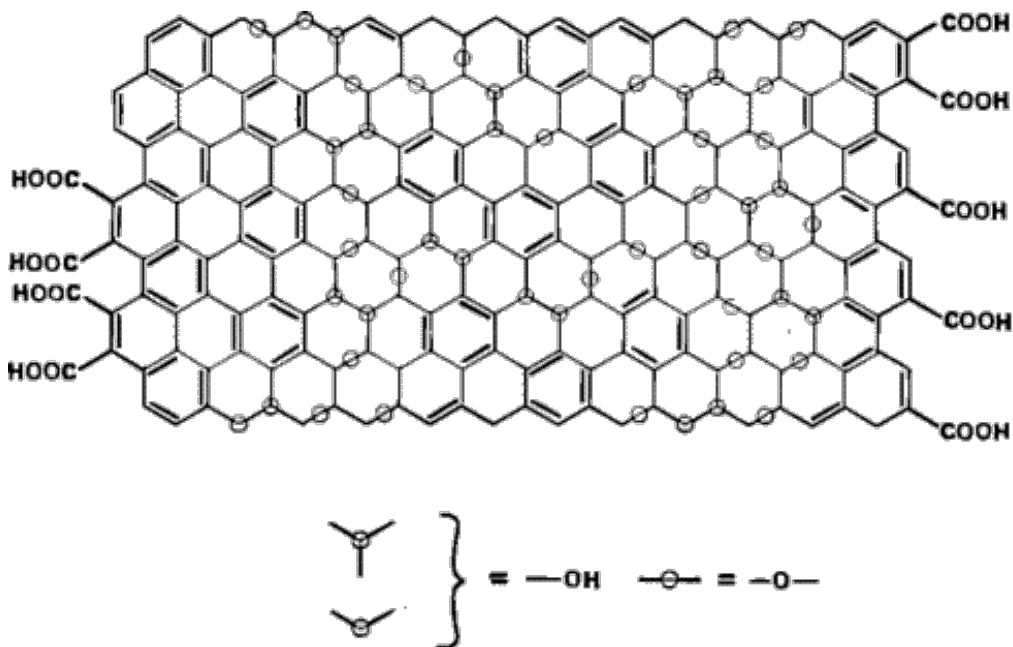


Figure 5.1 A proposed graphite oxide structure. Picture adopted from *J. Phys. Chem. B* 1998, **102**, 4477.

The intermediate to prepare chemically converted graphene is graphite oxide (Figure 5.1), which was discovered by Brodie in 1859 by oxidation of graphite [7]. However, in 2006 Ruoff's group was the first to demonstrate that graphite oxide can be reduced back to single layer graphene.[8] The graphitic  $sp^2$  networks are largely restored by chemical reduction or thermal annealing accompanied by the removal of oxygen. Despite the relatively low quality, graphite oxide can be easily chemically reduced to graphene and graphite oxide can be readily synthesized on a large scale. For example, in our lab, graphite oxide is prepared on the tens of grams scale for each batch. Graphite oxide is water soluble due to the oxygen containing groups (hydroxyl, epoxide and carboxyl), which interact strongly with water. However, the removal of oxygen during reduction makes the graphitic sheets hydrophobic and they aggregate quickly in water. Our group demonstrated that raising the pH during reduction could convert the carboxylic acid

groups into carboxylates and produce charge-stabilized colloidal graphene dispersions. [9] A graphene dispersion produced in this manner is stable for months without the need for surfactants or stabilizers.

Here a simple one-step approach to prepare solvothermal reduced graphite oxide (SRGO) that is dispersible in many organic solvents is demonstrated. Compared to other organic dispersible graphenes reported at the same time [10, 11], no surfactants or reducing reagents are used in the synthesis of SRGO. Thus, it does not suffer from the problem of eliminating the surfactant or the reducing reagent, which could be detrimental to many applications. This dispersible SRGO can be handled easily by common solution processing methods such as spray-on coating. It can also mix well with polymers that co-dissolve in the same solvent to produce homogeneous composites.

## **5.2 Experimental Section**

A 0.05 wt % GO dispersion in water was sonicated at 50 °C for 60 min using a VWR Ultrasonic Cleaner (B2500A-DTH, 210W) and diluted 1:1 with anhydrous NMP. The light brown dispersion obtained was then degassed for 60 min under vacuum to remove any residual atmospheric oxygen present in the mixture. The solution was then purged with argon and then refluxed for 24 h under flowing argon, after which it was filtered through an Anodisc alumina membrane filter (47 mm diameter, 0.2 µm pore size) and washed with pure NMP. The final product was centrifuged at 4500 rpm using a Beckman-Coulter Allegra X-15R centrifuge, saving the supernatant. The supernatant was filtered once again, rinsed with acetone, and allowed to dry on the filter paper under



ambient conditions, which will be referred to as the SRGO air-dried paper. Furthermore, several samples of SRGO paper were enclosed in a tube furnace under a flow of helium gas and annealed at temperatures of 250, 500, and 1000 °C. To make organic dispersions, SRGO paper was sonicated at a 1 mg/mL concentration in the following organic solvents for 3 h at 50 °C: dimethylsulfoxide (DMSO), ethyl acetate, acetonitrile, ethanol, tetrahydrofuran (THF), dimethylformamide (DMF), chloroform, acetone, toluene, and dichlorobenzene.

Atomic force microscopy (AFM) measurements were performed in tapping mode on a Multimode atomic force microscope (Nanoscope IIIa, Veeco Instruments) using a silicon tip. Samples were prepared using a 1 mg/mL solution of SRGO in DMF, which was drop-cast onto a freshly cleaned Si substrate and dried in the vacuum oven. Scanning electron microscope (SEM) analysis was carried out on both the SRGO papers and single sheets. Imaging of single sheets of SRGO and dispersions of SRGO were performed by depositing 1 mg/mL SRGO acetone onto a freshly cleaned Si substrate and allowing the acetone to evaporate.

X-ray diffraction (XRD) characterization was performed using SRGO air-dried paper on zero background silicon substrate in a Crystal Logic diffractometer with Ni-filtered Cu K $\alpha$  radiation ( $\lambda = 1.5418 \text{ \AA}$ ).

Thermal gravimetric analysis (TGA) of all samples was carried out under an argon gas and a heating rate of 2 °C/min.

Photoelectron spectroscopy (XPS) was performed by inserting samples into the analysis chamber of a Thermo VG ESCALAB 250 spectrometer. Spectra were obtained by irradiating each sample with a 320  $\mu\text{m}$  diameter spot of monochromated aluminum  $\text{K}\alpha$  X-rays at 1486.6 eV under ultrahigh vacuum conditions. The analysis consisted of acquiring 3–12 scans and signal averaging. The survey scans were acquired with a pass energy of 80 eV, and high-resolution scans were acquired with a pass energy of 20 eV.

The samples tested were obtained by filtering dispersions of SRGO directly from NMP after the solvothermal reaction to obtain a paper. The SRGO paper was then redispersed in acetone using sonication and filtered a second time to remove impurities. In addition to the solvothermally reduced GO, we also tested GO that had been reduced using the hydrazine reduction method.

Electrical measurements were performed using a four-point probe measurement station (Jandel RM3-AR Test Meter with Multiheight Probe attachment), and the average of three data points per sample was recorded.

### **5.3 Results and Discussion**

Filtered SRGO can be redispersed in many polar solvents. Stable colloidal dispersions can be achieved with dimethylsulfoxide (DMSO), ethyl acetate, acetonitrile, ethanol, tetrahydrofuran (THF), dimethylformamide (DMF), chloroform, and acetone with minimal precipitation at 1 mg/mL after 6 weeks. (Figure 5.2) SRGO does not disperse in

toluene or dichlorobenzene, but instead, flocculation was observed shortly after sonicating for 3 h. The solubility of graphene in different solvents can be explained based on solubility parameters. Park et al. have shown that highly reduced graphene oxide can be dispersed in solvents defined by  $10 < (\delta_p + \delta_h) < 30$ . [11]  $\delta_p$  is polarity cohesion parameter and  $\delta_h$  is hydrogen bonding cohesion parameter. They are two of the Hansen solubility parameters. Their data agree well with our results. Synthesis was carried out in DMF, DMSO, glycerol, and hexamethylphosphoramide (HMPA); however, agglomerated sheets form instead of colloidal dispersions. To our best knowledge, this can be explained by the cost of energy. NMP, unlike other solvents listed above, has a surface energy that closely matches that of exfoliated graphene. [12]

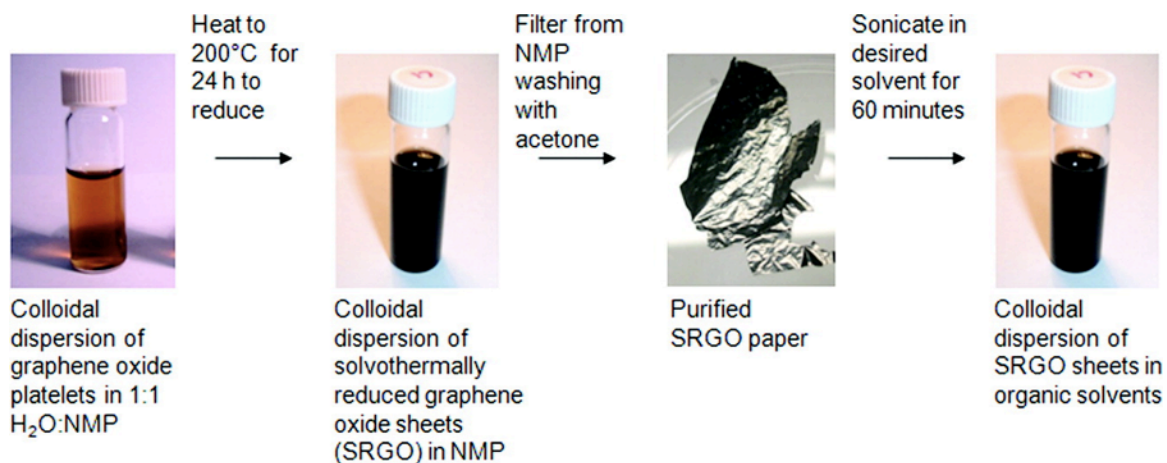


Figure 5.2 The preparation and purification of solvothermally reduced graphene oxide (SRGO) to create homogeneous colloidal dispersions of SRGO sheets.

Figure 5.3a shows AFM images of SRGO sheets deposited from a 1 mg/mL DMF dispersion onto a Si substrate. Figure 5.3b shows a 0.93 nm step height from the surface of the substrate to the sheet. This is higher than the theoretical step height for a single graphene sheet (0.34 nm). The increased step height may be attributed to residual

functionality on the surface of the sheet, causing some corrugation in the surface of the sheet. Figure 5.3c presents a scanning electron microscope (SEM) image of a 1 mg/mL acetone SRGO dispersion deposited onto a Si substrate. The image illustrates that the SRGO sheets are distributed across the Si substrate.

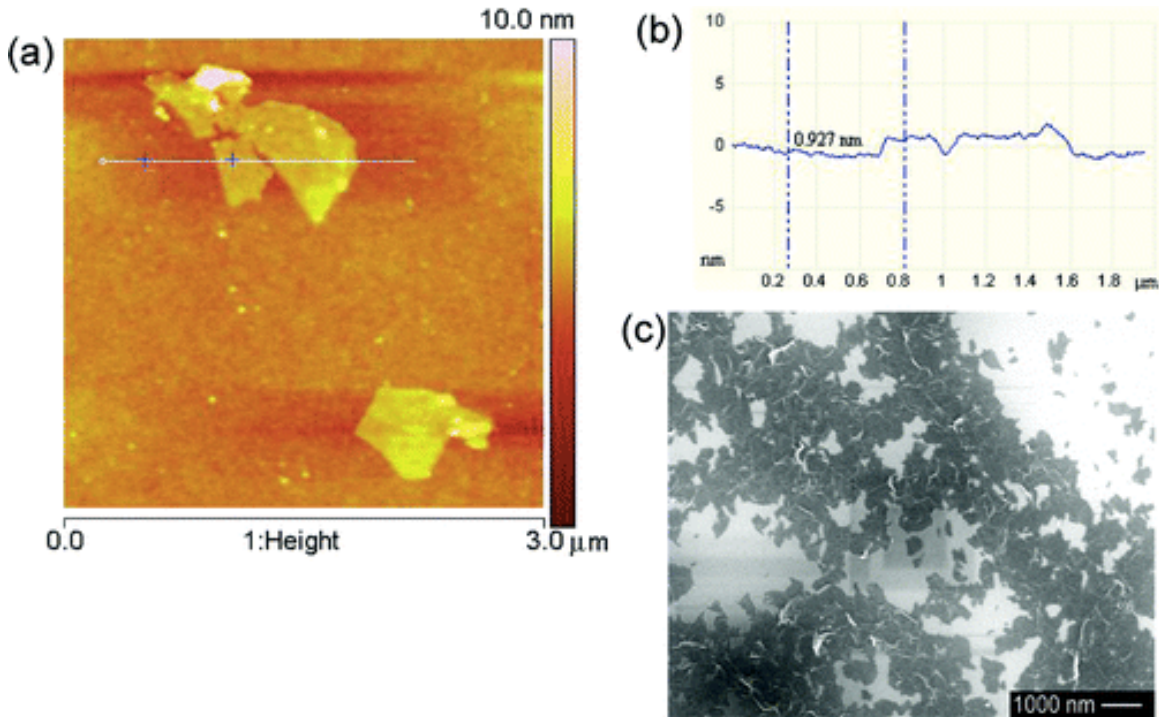


Figure 5.3(a) AFM image of SRGO sheets; (b) corresponding AFM height profile from (a) indicates a 0.93 nm sheet thickness. (c) SEM images of SRGO sheets indicate well-dispersed sheets after deposition on Si substrate; inset shows a highly magnified single sheet of SRGO.

XRD pattern (Figure 5.4a) of the GO paper exhibits a single peak at  $11.26^\circ 2\theta$  corresponding to an interlayer d spacing of 7.85 Å. The expansion of the 3.4 Å spacing between typical graphene sheets is resulted from the water molecules trapped between oxygen-containing functional groups on graphene oxide sheets. In contrast, the XRD pattern of SRGO shows a broad peak at  $26.24^\circ 2\theta$  (3.39 Å). The width of the SRGO peak

in the XRD pattern can be attributed to the small sheet size and a relatively short domain order. In Figure 5.4b, a TGA curve of the SRGO paper, in contrast, shows only 6% mass loss up to 200 °C whereas the GO paper shows a loss of about 15 wt % before 100 °C, signifying that a smaller amount of water molecules was trapped within the SRGO structure. Furthermore, the TGA of the SRGO paper shows a mass loss of 20% from 200 to 525 °C, which may be associated with strongly, bound NMP molecules.

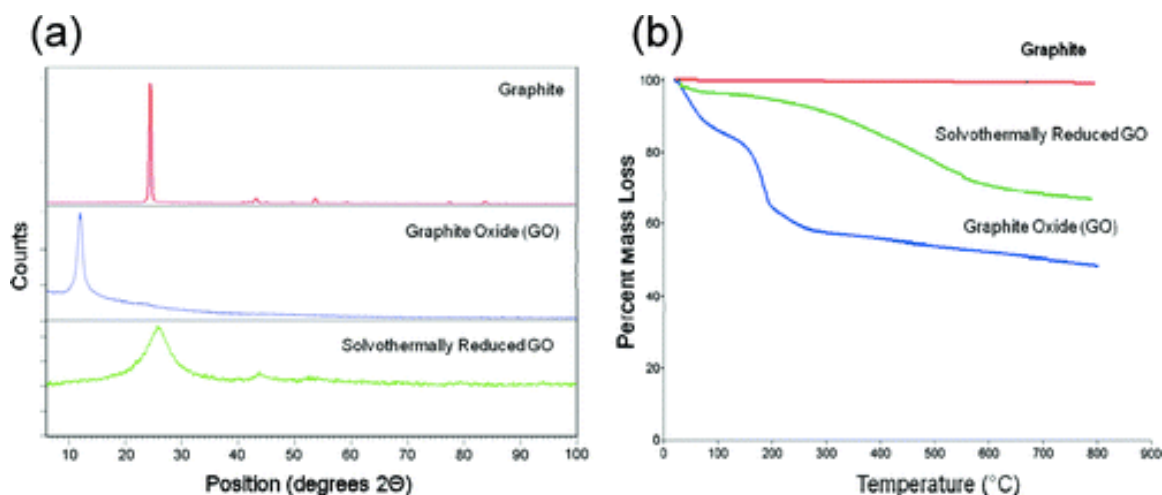


Figure 5.4 (a) XRD of graphite (top), graphite oxide (middle), reduced graphite oxide (bottom). (b) Thermal gravimetric analysis (TGA) plot shows a normalized remaining mass of graphite oxide, graphite, and reduced graphite oxide heated under argon.

Table 5.1 shows the electrical conductivity of SRGOs. Trapped residual NMP (boiling point = 203 °C) within the graphene sheets limits the conductivity of SRGO at room temperature. However, by annealing the sample to only 250 °C the conductivity is an order of magnitude higher. This indicates the removal of NMP, which improves the contacts between the graphene sheets. Further annealing to 500 °C and 1000 °C continues

to increase the conductivity, but at a slower rate. The conductivity after 1000 °C annealing is comparable to that of hydrazine reduced GO film.

Table 5.1 Electrical Conductivities SRGO Paper and Hydrazine Reduced Graphite Oxide

<b>description</b>	<b>drying conditions</b>	<b>conductivity (S/m)</b>
solvothermal RGO	air-dried	$3.74 \times 10^2$
	annealed at 250 °C	$1.38 \times 10^3$
	annealed at 500 °C	$5.33 \times 10^3$
	annealed at 1000 °C	$5.73 \times 10^4$
hydrazine RGO <sup>a</sup>	air-dried	$8.28 \times 10^3$
	annealed at 1000 °C	$6.67 \times 10^4$
GO boiled in H <sub>2</sub> O for 24 h	air-dried	$1.00 \times 10^1$
GO	air-dried	insulator

The reduction is also confirmed by XPS results. (Table 5.2) The C/O ratio increases from 2.34 to 5.15 after thermal reduction in NMP. Further annealing of SRGO papers at 1000 °C enhances the C/O ratio to 6.03. C/O ratio of hydrazine reduced GO is 3.64. When the hydrazine RGO papers were annealed at 1000 °C, the C/O ratio reaches up to 6.36. Although the C/O ratio of SRGO is higher before annealing, the increase is most likely due to bound NMP molecules and not an improved de-oxygenation. When SRGO and hydrazine RGO are annealed, both reduction methods exhibited similar C/O ratios, with hydrazine RGO having a slightly higher ratio over SRGO. The result of the XPS data agrees with the electrical conductivity data.

Table 5.2 Atomic Compositions of SRGO and Hydrazine RGO Measured by XPS

description	drying conditions	C (atomic %)	O (atomic %)	N (atomic %)	C/O ratio
solvothermal RGO	air-dried	80.4	15.6	4.0	5.15
solvothermal RGO	annealed at 1000 °C	83.2	13.8	3.0	6.03
hydrazine RGO <sup>a</sup>	air-dried	76.0	21.0	3.0	3.62
hydrazine RGO <sup>a</sup>	annealed at 1000 °C	84.5	13.3	2.2	6.36
GO boiled in H <sub>2</sub> O for 24 h	air-dried	75.4	21.1	0.5	3.12
GO	air-dried	69.3	29.3	1.1	2.34

## 5.4 Conclusions

Thermally reduced graphite oxide can be produced in NMP without the aid of any surfactant and/or reducing agent. The SRGO can form good dispersions in various solvents. Although the conductivity is slightly lower than a hydrazine reduced graphene dispersion, it's suitable for organic solvent-based applications. Post treatment of SRGO films can also improve the conductivity even further.

## 5.5 References

1. P. R. Wallace, *Phys. Rev.* **1947**, 71, 623.
2. Novoselov, K. S., Geim, A. K., Morozov, S. V., Jiang, D., Zhang, Y., Dubonos, S. V., Grigorieva, I. V. and Firsov, A. A. *Science* **2004**, 306, 666.
3. Novoselov, K. S., McCann, E., Morozov, S. V., Fal'ko, V. I., Katsnelson, M. I., Zeitler, U., Jiang, D., Schedin, F. and Geim, A. K. *Nat. Phys.* **2006**, 2, 177.
4. Jiang, Z., Zhang, Y., Stormer, H. L. and Kim, P. *Phys. Rev. Lett.* **2007**, 99, 106802.
5. Novoselov, K. S., Geim, A. K., Morozov, S. V., Jiang, D., Katsnelson, M. I., Grigorieva, I. V., Dubonos, S. V. and Firsov, A. A. *Nature* **2005**, 438, 197.
6. Morozov, S. V., Novoselov, K. S., Katsnelson, M. I., Schedin, F., Elias, D. C., Jaszczak, J. A. and Geim, A. K. *Phys. Rev. Lett.* **2008**, 100016602.
7. Brodie, B. C. *Philos. Trans. R. Soc. London* **1859**, A149, 249.
8. Stankovich, S., Dikin, D. A., Dommett, G. H. B., Kohlhaas, K. M., Zimney, E. J., Stach, E. A., Piner, R. D., Nguyen, S. T. and Ruoff, R. S. *Nature* **2006**, 442, 282.
9. Li, D., Muller, M. B., Gilje, S., Kaner, R. B. and Wallace, G. G. *Nat. Nanotechnol.* **2008**, 3, 101.
10. Yanyu Liang, Dongqing Wu, Xinliang Feng and Klaus Mullen, *Adv. Mater.* **2009**, 21, 1679.
11. Sungjin Park, Jinho An, Inhwa Jung, Richard D. Piner, Sung Jin An, Xuesong Li, Aruna Velamakanni, and Rodney S. Ruoff, *Nano. Lett.* **2009**, 9, 1593.
12. Hernandez, Y.; Nicolosi, V.; Lotya, M.; Blighe, F. M.; Sun, Z.; De, S.; McGovern, I. T.; Holland, B.; Byrne, M.; Gun'Ko, Y. K. *Nat. Nanotechnol.* **2008**, 3, 56